An Atomistic Solution: Semiconductors Growth, Material & Device Characterization

Technology of Next Level
driven through innovation

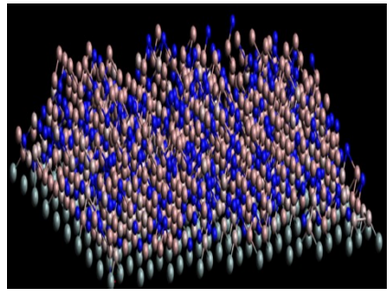

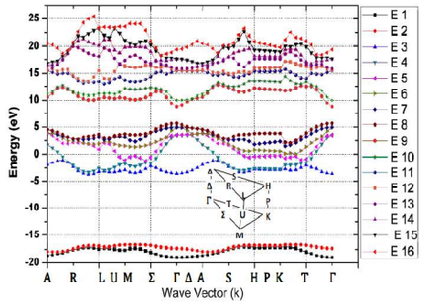

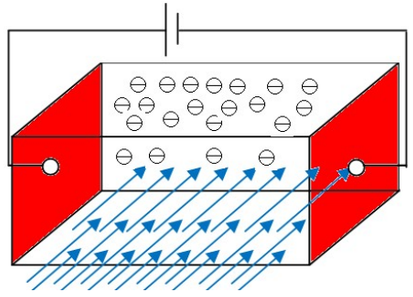

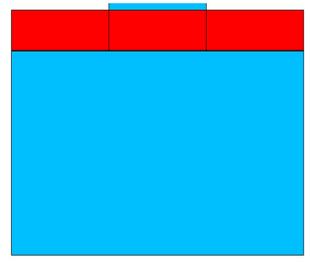

COMPANY OVERVIEW

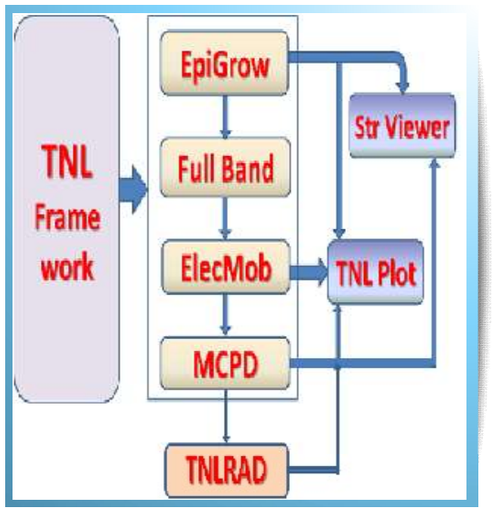

Atomistic TCAD Full Flow

Radiation Monitoring System

Night Vision & Border Surveillance

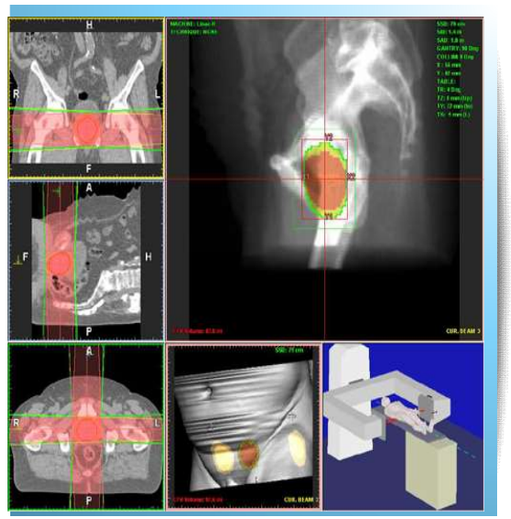

Medical Radiation Dosimetry

Core Team Members

TCAD Expert
Experience 15 years

Praveen Saxena
Founder & CEO

Material Scientist
Experience 10+ years

Pankaj Srivastava
CPO

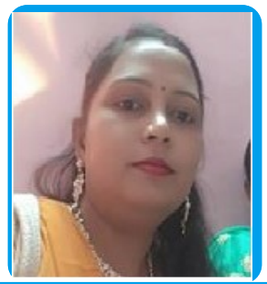

Software Engineering
7+ years

Anshu Saxena
Cofounder & Director

Nuclear Scientist
3+ years

Anshika Srivastava
Manager

Device Expert
3+ years

Fanish Gupta
Manager

ATOMISTIC TCAD TOOLS

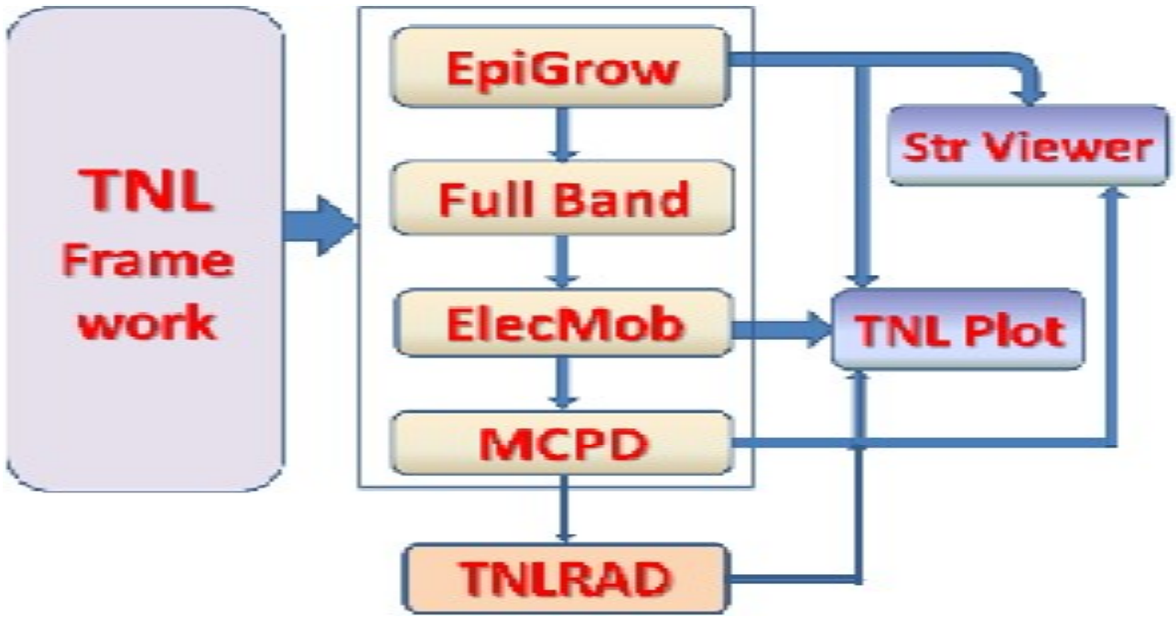

- ❑ Epitaxial Growth Process
- ❑ Material Characterization
- ❑ Material Characterization
- ❑ Particle based Device
- ❑ Impact of Radiation / High Frequency EM waves (under Development)

CRYSTAL GROWTH

Epitaxial Growth of Group IV, III-V & II-VI Semiconductors

CRYSTAL GROWTH

1. Bulk Crystal Growth

❑ State of the art device technologies depends on: **Purity & Perfection of the crystals**

❑ Limited to **Si, GaAs** and upto some extent for **InP**

Silicon

- Available in up to >30 cm diameter
- Quite inexpensive and high quality
- Can be obtained *n*-type, *p*-type, or with high resistivity
- Used for Si and SiGe technologies
- Intense reserach to develop Si-based "pseudo-substrates" for GaAs, InP, CdTe...technologies

GaAs

- Available in up to >12 cm diameter
- High quality, more expensive than Si, but affordable
- Used for GaAs and AlGaAs, and strained InGaAs technologies
- Can be used for electronic and optoelectronic applications

InP

- 10 cm diameter available, but expensive
- InP and InGaAsP technologies can be grown
- Very important for optoelectronics and high performance electronics

SiC

- Small, very expensive substrates
- Very important for high power, large gap technologies
- Used for nitride technology

EPITAXIAL GROWTH CHALLENGES

❑ **Development of psuedo-substrates**

Substrate B
Buffer layer
Substrate A

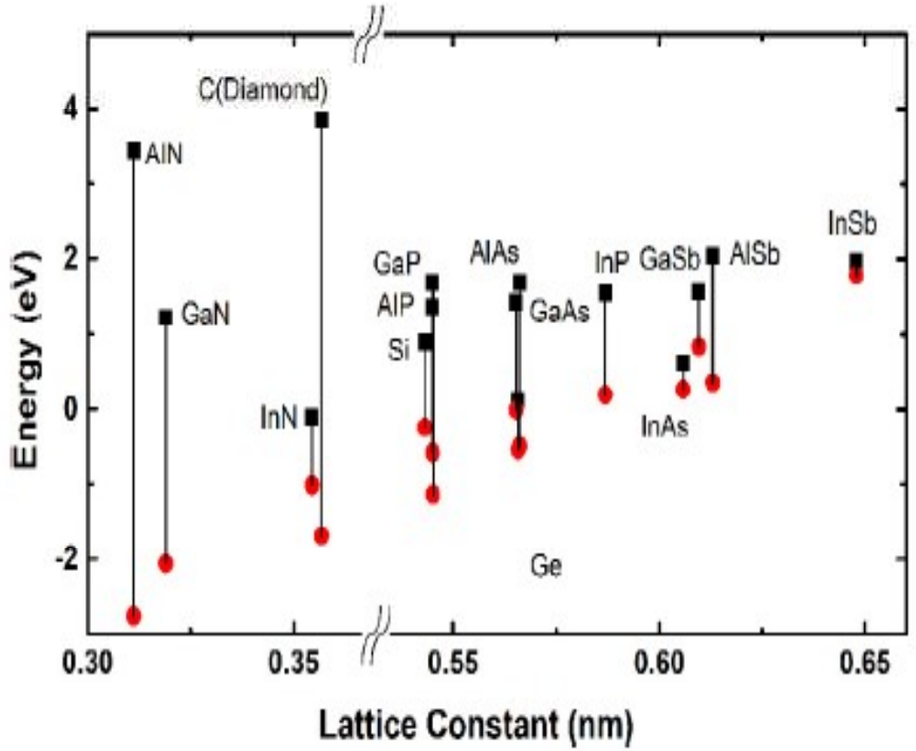

*E.T. Yu, J.O. McCaldin, T.C. McGill, Band offsets in semiconductor heterojunctions, in: E. Henry, T. David (Eds.), Solid State Physics, Academic Press, 1992, pp. 1–146

CRYSTAL GROWTH

2. Epitaxial Growth

- ❑ Semiconductor technologies dependent on non ideal substrates
- ❑ Lot of Technological Challenges

LPE

- Very high quality material
- Near equilibrium growth for precise alloy compositions
- Relatively inexpensive
- Difficult to grow abrupt heterostructures
- Unable to grow immiscible alloys

VPE

- Extremely high purity material
- Not well suited for heterostructures

(MBE) (MOCVD) (MOMBE)

- High quality material
- Atomically abrupt interfaces
- Techniques can grow far from equilibrium systems reliably

Expensive growth technology ????

TNL

EPITAXIAL GROWTH CHALLENGES

- Group IV, III-V, II-VI epi-growth due to multi components of the growth system
- Point defects, e.g. vacancies, interstitial atoms, impact on the performance of the device
- Extended defects within the film are generally dislocations and stacking faults
- Dislocations can reduce or relax strain introduced through lattice mismatch or thermal expansion differences.

GaN growth over:

Substrate	Si	Al_2O_3	SiC	Bulk GaN	AlN
Lattice Mismatch (%)	17	16	3.4	-	2.5
Thermal Conductivity (W/mm-k)	150	35	490	260	319
Resistivity (ohm-cm)	10^4	10^{14}	~10^{12}	-	>10^{14}

EPITAXIAL GROWTH CHALLENGES

Defects

- ❑ Edge Dislocation
- ❑ Vacancies
- ❑ Interstitial
- ❑ Grain Boundaries

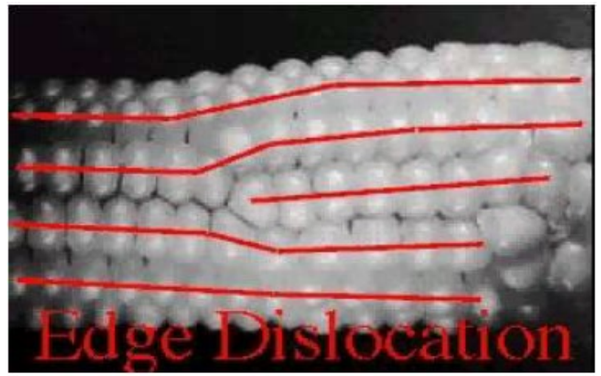

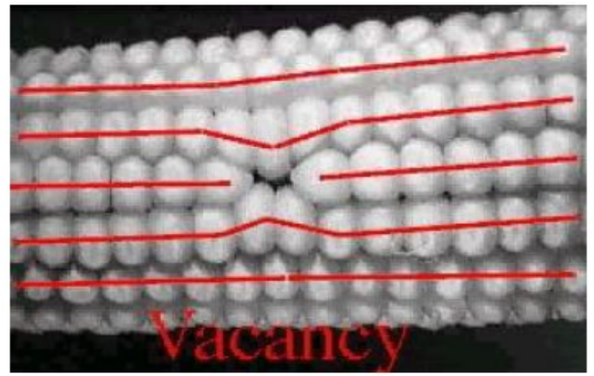

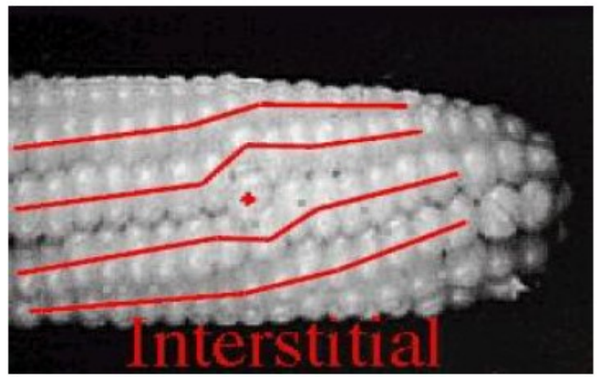

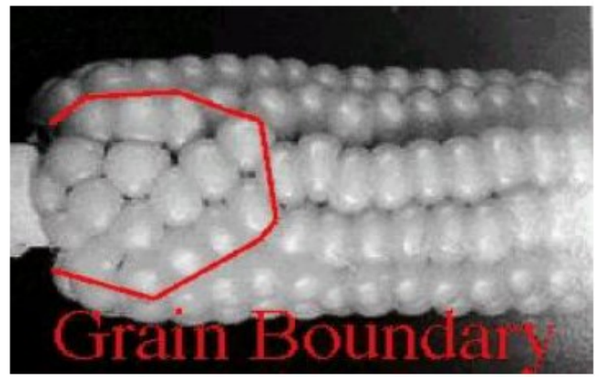

Chungnam Natl Univ., S. K. Hong

TNL

EPITAXIAL GROWTH CHALLENGES

- **Empirical relations procedures, difficult to use if the reactants or the reactor geometry is change**
- **Statistical methods create purely empirical models of reactor behavior**
- **Mathematical modeling and simulation provide upto some extend economic alternative to trial and error-based experimental techniques**
- **To fulfill the increasing demand by the industry: epiwafer supplies very difficult and time-consuming tasks**
- **Lack of detailed fundamental models has forced industrial CVD practitioners to rely on methods of trial and error: Expensive**

EpiGrow Simulator

Innovative Atomistic Reactor Simulation

Inbuilt Reactors

- MBE
- MOCVD
- GasMBE
- CVD & PVD (under development)

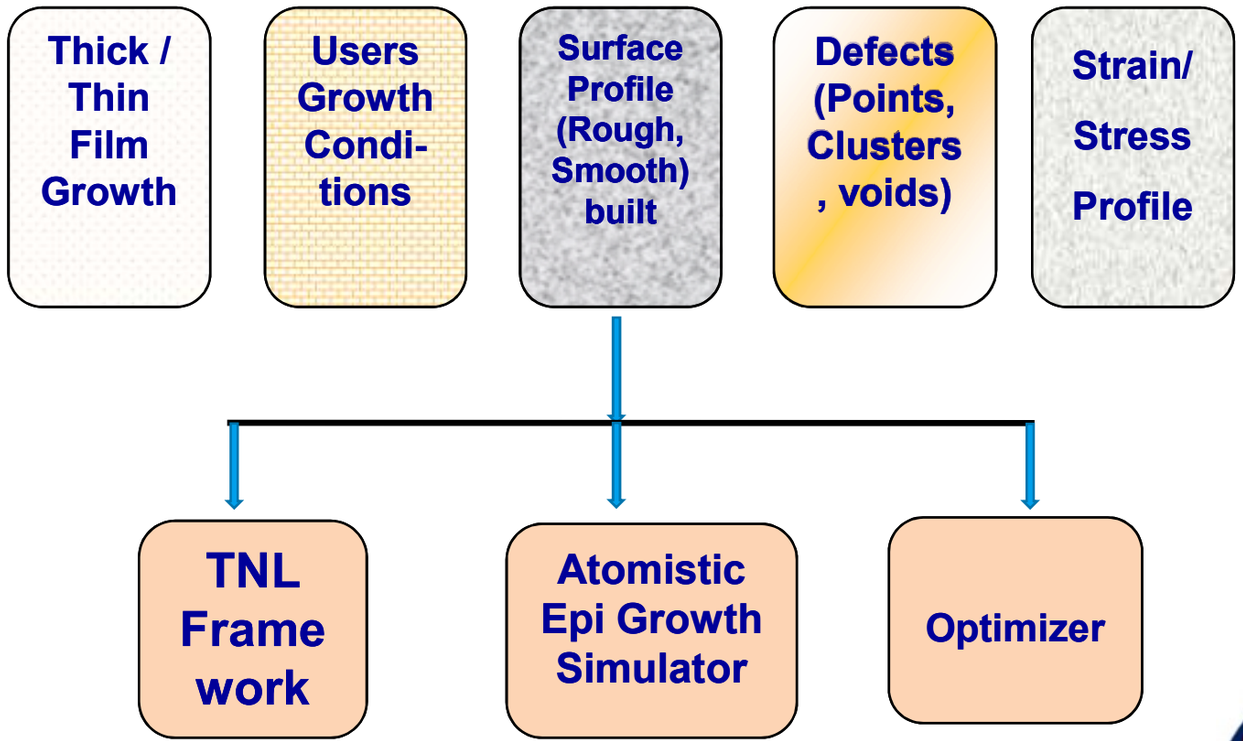

EpiGrow Simulator

Benefits can be realized

- ❑ Users growth conditions
- ❑ Surface profiles Extracting Roughness
- ❑ Defects Extraction (point/clusters)
- ❑ Extraction of dislocations & Stress/ Strain
- ❑ Fewer experiments for optimization
- ❑ Reduction in waste during experimentation
- ❑ Ability to deal with different reactive species and reactor geometries
- ❑ On-line process control

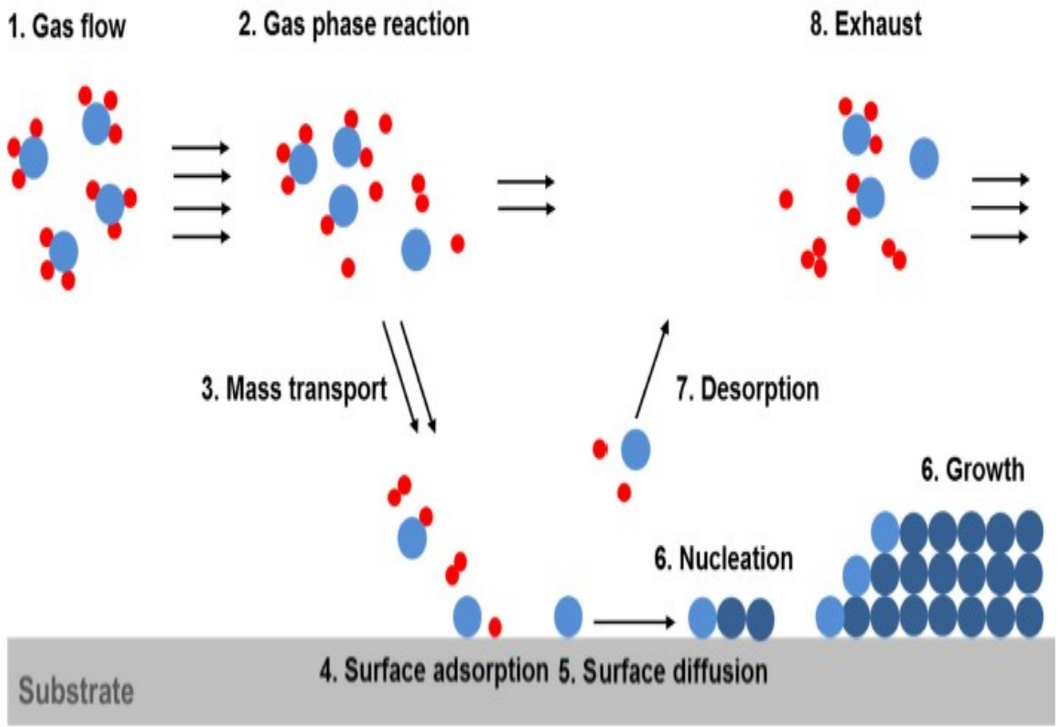

EpiGrow Simulator

❑ **Schwoebel barrier:** The atom diffuses from the site exactly above the edge atom to the site immediately next to the edge atom,

❑ **Incorporation barrier:** The atom incorporates into the edge on the same surface level.

❑ **Strain:** ➡ $(a - a_0) / a_0$

❑ **Sticking coefficient** ➡ $s_c = P_{ads}(1-m)\sum_{n=0}^{\infty} P_{hop}^{n}$

❑ **Total Rates** $R_T = R_{ads} + R_{hop} + R_{des}$

Here ads ~ adsorption Rate on substrate , Hop ~ hopping rate on substrate
Des ~ desorption rate

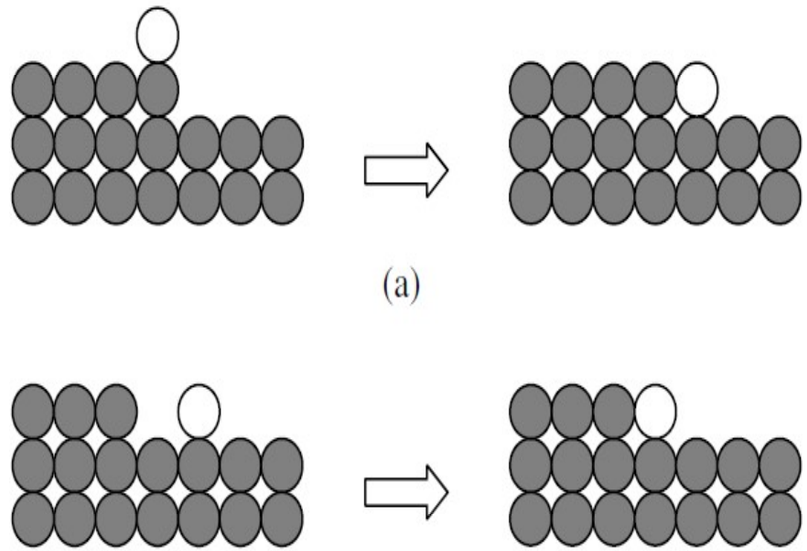

Side view for the case of Schwoebel barrier (a) and that of incorporation barrier (b), where the white atom is the diffusing one.

GaAs/GaN: MBE EpiGrowth

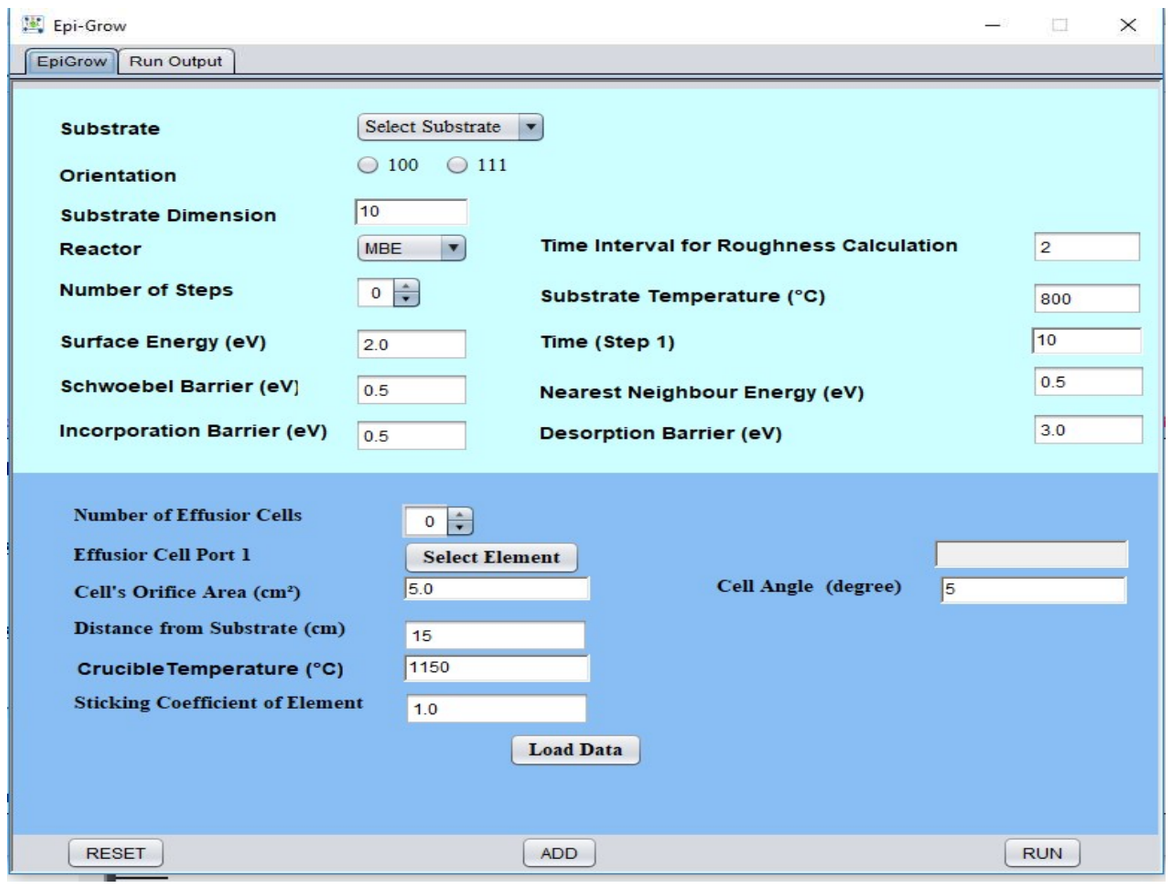

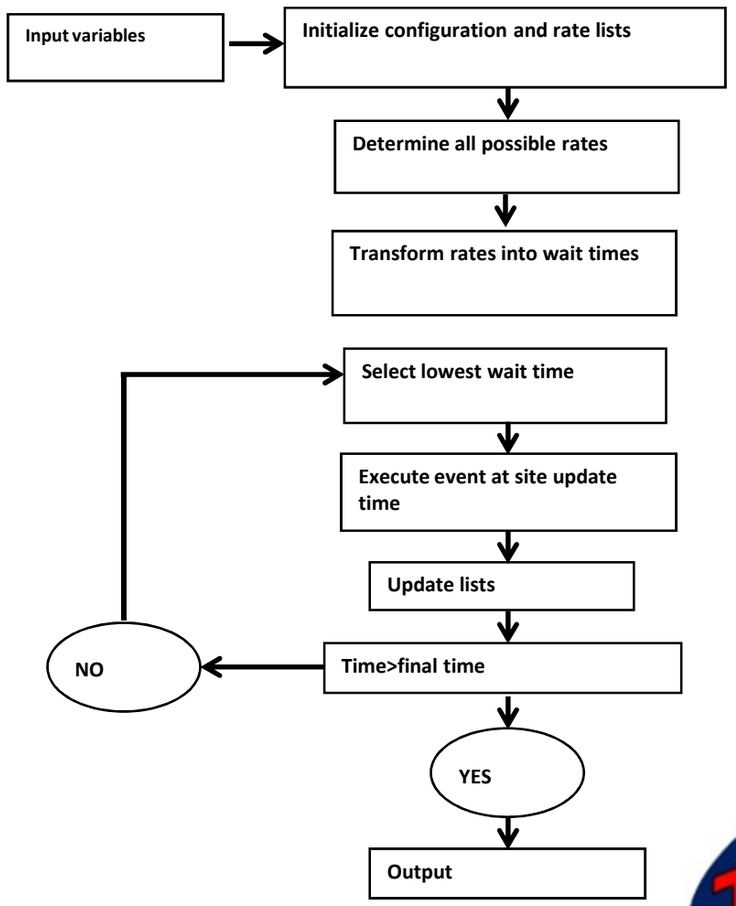

GaAs/GaN: MOCVD EpiGrowth

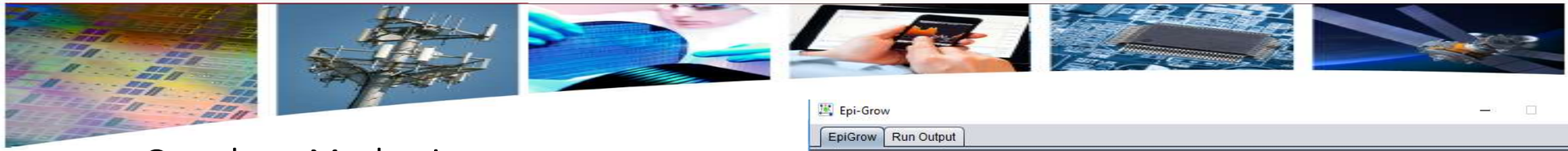

Gas-phase Mechanisms:

										$k = AT^n e^{-Ea/RT}$		
										A	n	E_a
G1	TMG	=	DMG	+	CH_3					1.00×10^{47}	−9.18	76,996
G2	DMG	=	MMG	+	CH_3					7.67×10^{43}	−9.8	34,017
G3	MMG	=	Ga	+	CH_3					1.68×10^{30}	−5.07	84,030
G4	TMG	+	NH_3	→	TMG:NH_3					2.28×10^{34}	−8.31	3115
G5	TMG	+	NH_3	→	DMG:NH_2	+	CH_4			1.70×10^{4}	2	19,969
G6	DMG	+	NH_3	→	DMG:NH_3					4.08×10^{31}	−7.03	3234
G7	DMG	+	NH_3	→	MMG:NH_2	+	CH_4			5.30×10^{5}	1.56	20,744
G8	MMG	+	NH_3	→	MMG:NH_3					7.95×10^{24}	−5.21	2094
G9	MMG	+	NH_3	→	$GaNH_2$	+	CH_4			8.10×10^{5}	1.3	17,722
G10	NH_3	+	CH_3	→	NH_2	+	CH_4			3.31×10^{3}	2.51	9859
G11	CH_3	+	H_2	→	CH_4	+	H			1.20×10^{12}	0	12,518
G12	TMG	+	H	→	DMG	+	CH_4			5.00×10^{13}	0	10,036
G13	DMG	+	H	→	MMG	+	CH_4			5.00×10^{13}	0	10,036
G14	TMG:NH_3	→	MMG	+	$2CH_3$	+	NH_3			1.33×10^{44}	−8.24	77,791
G15	CH_3	+	H	+	M	→	CH_4	+	NH_3	2.40×10^{22}	−1	0
G16	$2CH_3$	=	C_2H_6							2.00×10^{13}	0	0
G17	2H	+	M	=	H_2	+	M			2.00×10^{16}	0	0

Surface phase Mechanisms:

	Path 1, $k = AT^n e^{-Ea/RT}$								A	n	E_a
1	MMG	+	N(S)	→	MMG(S)				1.16×10^{5}	2.98	0
2	MMG(S)	→	MMG	+	N(S)				1.12×10^{14}	0.55	107,673
3	NH_3	+	MMG(S)	→	COMPM1(S)				3.35×10^{7}	3.33	0
4	COMPM1(S)	→	NH_3	+	MMG(S)				5.70×10^{13}	−0.16	8146
5	MMG	+	COMPM1(S)	→	CH4	+	COMPM2(S)		1.23×10^{10}	3.22	23,446
6	NH_3	+	COMPM2(S)	→	COMPM3(S)				3.35×10^{7}	3.33	0
7	COMPM3(S)	→	NH_3	+	COMPM2(S)				5.70×10^{13}	−0.161	8146
8	MMG	+	COMPM3(S)	→	CH4	+	COMPM4(S)		1.23×10^{10}	3.22	23,446
9	NH_3	+	COMPM4(S)	→	COMPM5(S)				3.35×10^{7}	3.33	0
10	COMPM5(S)	→	NH_3	+	COMPM4(S)				5.70×10^{13}	−0.161	8146
11	COMPM5(S)	→	CH4	+	RINGM1(S)				1.23×10^{7}	3.22	23,446
12	Ga(S)	+	RINGM1(S)	→	RINGM2(S)	+	N(S)		3.35×10^{7}	3.33	0
13	RINGM2(S)	→	$3H_2$	+	3GaN(B)	+	Ga(S)		3.68×10^{9}	2.05	59,610

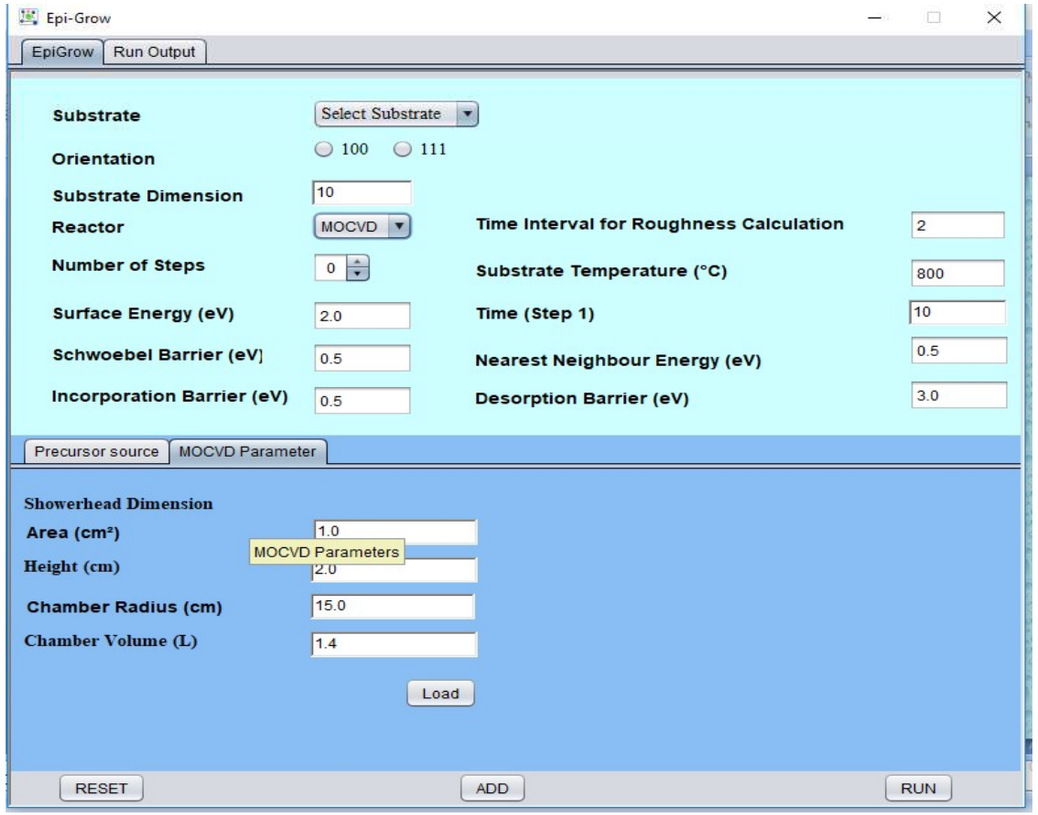

GaN: MOCVD EpiGrowth

Surface phase Mechanisms: PATH 2

			Path 2, $k = AT^n e^{-Ea/RT}$				A	n	E_a
14	CH_3	+	Ga(S)	→	MMG(S)		1.76×10^9	1.39	0
15	MMG(S)	→	CH_3	+	Ga(S)		4.54×10^{13}	0.0346	79,480
16	NH_2	+	Ga(S)	→	NH_2(S)		3.17×10^8	1.83	0
17	$GaNH_2$	+	N(S)	→	$GaNH_2$(s)		2.27×10^6	2.247	0
18	$GaNH_2$(S)	→	$GaNH_2$	+	N(S)		4.83×10^{13}	0.614	83,881
19	COMPMM1(S)	→	CH_4	+	$GaNH_2$(S)		1.49×10^{11}	0.609	25,950
20	MMG	+	$GaNH_2$(S)	→	COMPMM1(S)		1.16×10^5	2.98	0
21	NH_3	+	COMPMM1(S)	→	COMPMM2(S)		3.35×10^7	3.33	0
22	COMPMM2(S)	→	CH_4	+	COMPMM3(S)		1.49×10^{11}	0.609	25,950
23	MMG	+	COMPMM3(S)	→	COMPMM4(S)		1.16×10^5	2.98	0
24	NH_3	+	COMPMM4(S)	→	COMPMM5(S)		3.35×10^7	3.33	0
25	COMPMM5(S)	→	CH_4	+	RINGM1(S)		1.49×10^{11}	0.609	25,950
26	NH_2(S)	→	NH_2	+	Ga(S)		1.45×10^{14}	0.09	59,786
27	COMPMM1(S)	→	MMG	+	$GaNH_2$(S)		1.00×10^{14}	0.55	42,819
28	COMPMM2(S)	→	NH_3	+	COMPMM1(S)		5.70×10^{13}	−0.1	8146
29	COMPMM4(S)	→	MMG	+	COMPMM3(S)		1.00×10^{14}	0.55	42,819
30	COMPMM5(S)	→	NH_3	+	COMPMM4(S)		5.70×10^{13}	−0.1	8146
31	Ga	+	N(S)	→	Ga(S)		1.00×10^{11}	1.5	0
32	Ga(S)	+	NH_2(S)	→	$GaNH_2$	+Ga(S)	1.00×10^{25}	0	0
33	Ga(S)	→	Ga	+	N(S)		1.00×10^{13}	0	45,168
34	$6CH_3$	+	RINGM2(S)	→	COM1(S)		7.55×10^7	2.31	0
35	COM1(S)	→	$6CH_3$	+	RINGM2(S)		1.00×10^{13}	0.71	45,506
36	COM1(S)	→	$6CH_4$	+	3GaN(B)	+Ga(S)	4.00×10^{12}	0	49,675

Surface phase Mechanisms: PATH 3

				Path 3, $k = AT^n e^{-Ea/RT}$				A	n	E_a
37	TMG	+	N(S)	→	TMG(S)			1.16×10^5	2.98	0
38	NH_3	+	TMG(S)	→	TCOM1(S)			3.35×10^7	3.33	0
39	TCOM1(S)	→	CH_4	+	TCOM2(S)			1.49×10^{11}	0.609	32,785
40	Ga(S)	+	TCOM2(S)	→	TCOM3(S)	+	N(S)	3.35×10^7	3.33	0
41	TCOM3(S)	→	$2CH_4$	+	GaN(B)	+	Ga(S)	1.49×10^{11}	0.609	49,675
42	TMG(S)	→	TMG	+	N(S)			1.12×10^{14}	0.55	49,675
43	TCOM1(S)	→	NH_3	+	TMG(S)			5.70×10^{13}	−0.161	11,922
44	TMG:NH_3	+	N(S)	→	TCOM1(S)			1.16×10^5	2.98	0
45	TCOM1(S)	→	TMG:NH_3	+	N(S)			1.12×10^{14}	0.55	49,675
46	TCOM1(S)	→	$2CH_3$	+	MMG(S)	+	NH_3 +N(S)	1.12×10^{14}	0.55	10,7673
47	MMGNH_3	+	N(S)	→	COMPM1(S)			1.16×10^5	2.98	0
48	COMPM1(S)	→	MMG:NH_3	+	N(S)			1.12×10^{14}	0.55	107,673
49	MMG:NH_3	+	COMPM1(S)	→	CH_4	+	COMPM3(S)	1.23×10^{10}	3.22	23,446
50	MMG:NH_3	+	COMPM3(S)	→	CH_4	+	COMPM5(S)	1.23×10^{10}	3.22	23,446
51	MMG:NH_3	+	$GaNH_2$(S)	→	COMPMM2(S)			1.16×10^5	2.98	0
52	MMG:NH_3	+	COMPMM3(S)	→	COMPMM5(S)			1.16×10^5	2.98	0

Chemical Composition of compound on the surface

Compounds Names	Chemical Formula
COMPM1(S)	NH_3·MMG(S)
COMPM2(S)	Ga·NH_2·MMG(S)
COMPM3(S)	NH_3·Ga·NH_2·MMG(S)
COMPM4(S)	Ga·NH_2·Ga·NH_2·MMG(S)
COMPM5(S)	NH_3·Ga·NH_2·Ga·NH_2·MMG(S)
RINGM1(S)	NH_2·Ga·NH_2·Ga·NH_2·Ga(S)
RINGM2(S)	(S)NH_2·Ga·NH_2·Ga·NH_2·Ga(S)
COMPMM1(S)	MMG·$GaNH_2$(S)
COMPMM2(S)	NH_3·MMG·$GaNH_2$·Ga(S)
COMPMM3(S)	NH_2·Ga·NH_2·Ga(S)
COMPMM4(S)	MMG·NH_2·Ga·NH_2·Ga(S)
COMPMM5(S)	NH_3·MMG·NH_2·Ga·NH_2·Ga(S)
TCOM1(S)	NH_3·TMG(S)
TCOM2(S)	NH_2·DMG(S)
TCOM3(3)	(S)NH_2·DMG(S)
COM1(S)	RINGM2(S)·CH_3 complex

OUTPUT Results

1. Lattice Constant :

- ❑ Layer by layer lattice constant Extraction.
- ❑ Averaging layer by layer lattice constant may produce overall lattice constant of film.
- ❑ The lattice constant can be calibrated with XRD studies obtained lattice constant .
- ❑ Lattice constant includes all the strain, defects etc effects.

2. Strain:

- ❑ Averaging layer by layer strain will produce overall strain in the film.
- ❑ The strain can be calibrated with experimental strain.

3. Surface Roughness:

- ❑ User may extract surface roughness w.r.t time, included through

$$r = \sqrt{\frac{\sum_{i=1}^{N}\sum_{j=1}^{N}[h_{ij}-\bar{h}]^2}{NxN}}$$

Here N is the total number of lattice points, h_{ij} is the height at a given lattice point located at position *i* and *j*, on the lattice and h_{avg} is the average height of all lattice points.

4. Mole fraction:

- ❑ User may extract number of atoms of different constituents layer by layer.
- ❑ Ratio of group-III & V atoms, molefraction can be produced.

5. Defects :

- ❑ User may extract number of interstitials, vacancy etc layer by layer

Case Study

Controlled Epitaxial Growth of GaAs in real MOCVD Reactor Environment*

*P. K. Saxena, P. Srivastava, R. Trigunayat, An innovative approach for controlled epitaxial growth of GaAs in real MOCVD reactor environment, *Journal of Alloys and Compounds* 809 (2019) 151752.

GaAs: MOCVD EpiGrowth

GaAs monolayers growth over GaAs

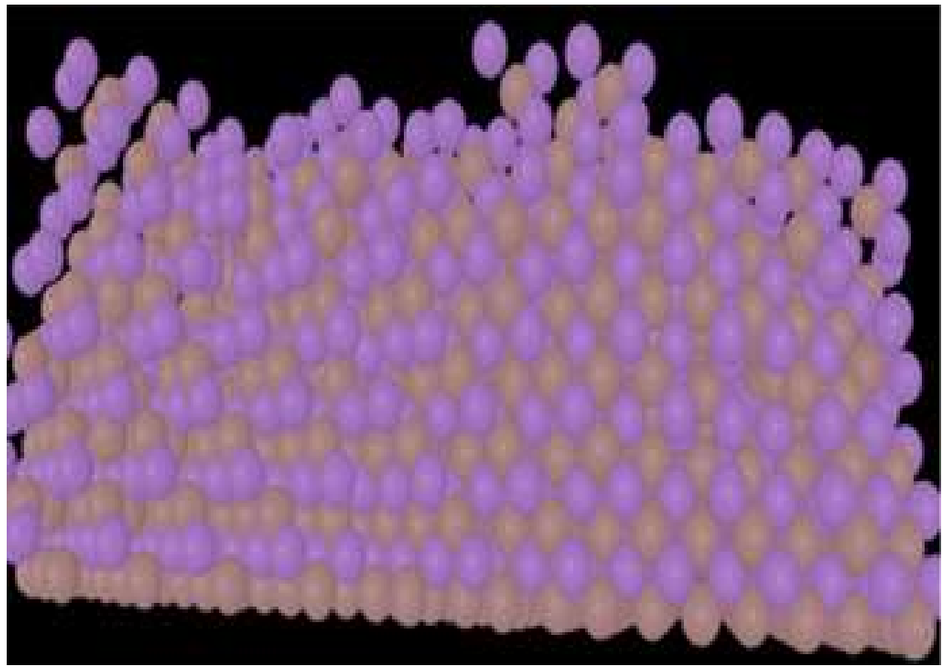

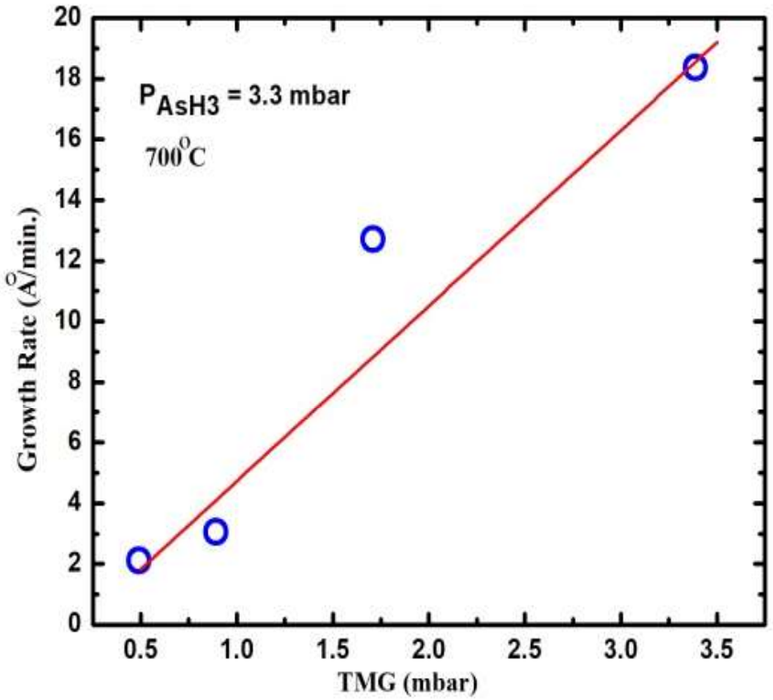

* Journal of Alloys and Compounds 809 (2019) 151752.

GaAs: MOCVD EpiGrowth

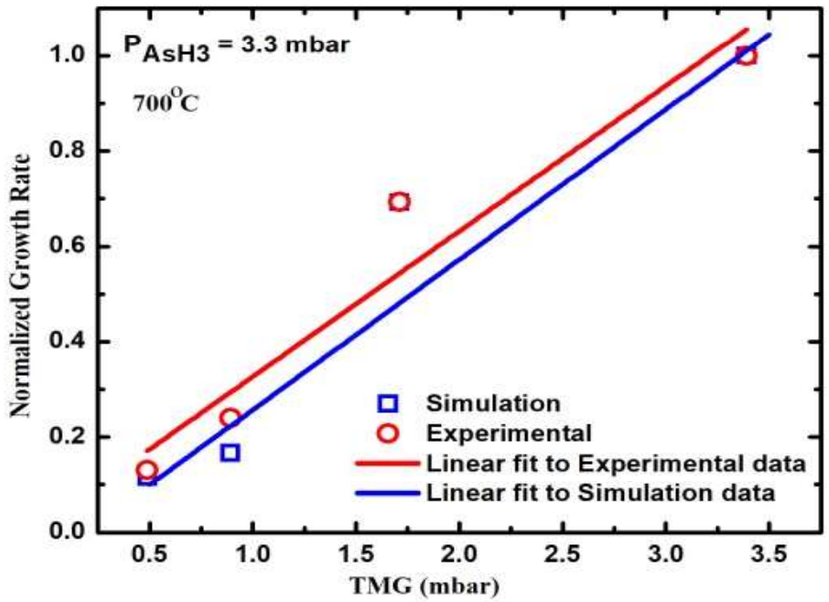

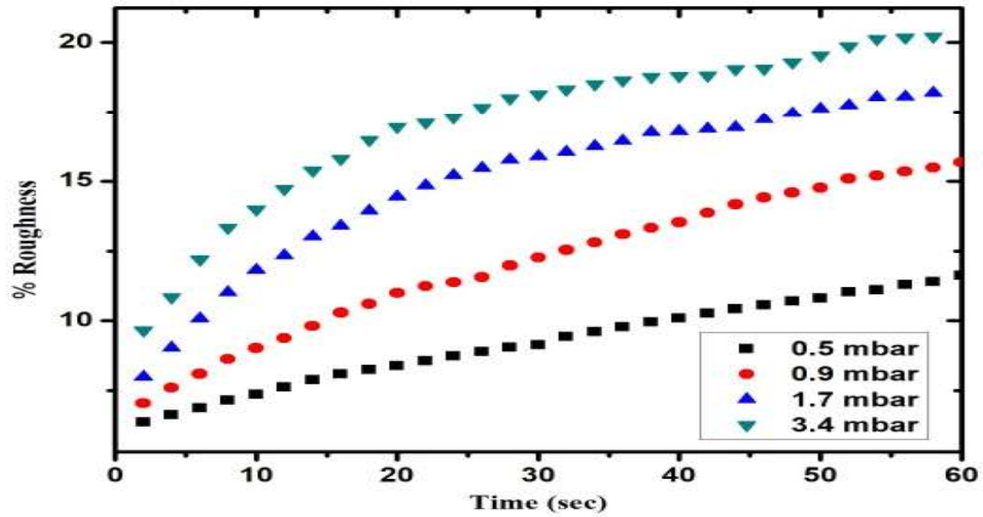

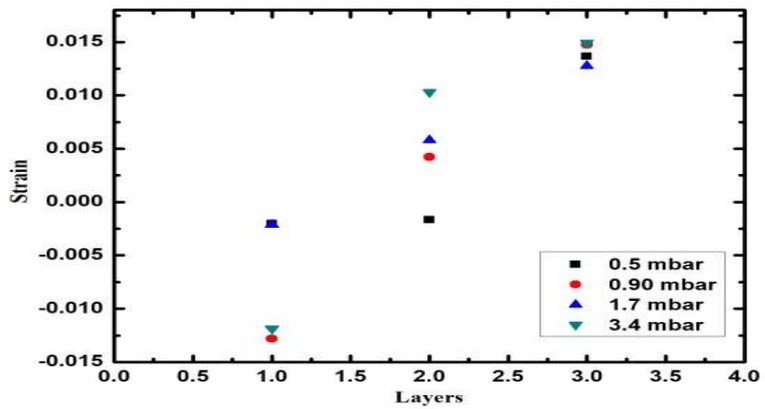

[* Journal of Alloys and Compounds 809 (2019) 151752.]

Material Characterization of thin/thick Film

Full Band Structure

- Electronic band structure of IV, III-V and II-VI alloys using standard lattice constant “a”
- Virtual Crystal Approximation for ternary alloys.
- Semi-empirical disorder contribution.
- Non-Parabolicity & Parabolicity effects
- Main valleys energies, effective masses with non-parabolicity factors, carrier group velocity, DOS etc.

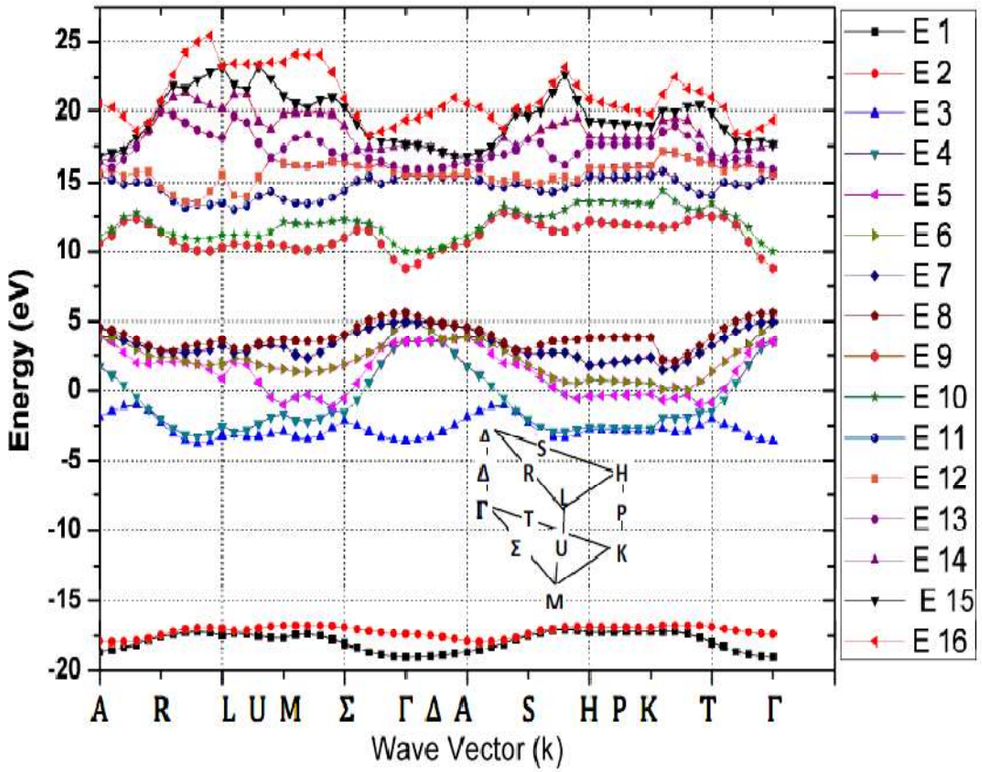

Case Studies

Material Characterization through Electronic Transport on Band Structure

***** Praveen K Saxena *at. el.,* An Innovative Model for Electronic Band Structure Analysis of doped and un-doped ZnO, *Journal of Electronic Materials Accepted for publication.*

*****Anshika Srivastava, Anshu Saxena, Praveen K. Saxena, F. K.Gupta, Priyanka Shakya, *at. el.***,** An innovative technique for electronic transport model of group-III nitrides, ***Scientific Reports nature research*** (2020) **10**:18706.

ZnO: Full Band Simulator

Different DFT based calculated energy band gap of ZnO materials within the conventional DFT (LDA and PBE functional), LDA + U functional, and hybrid functional (HSE06) along with the lattice parameters, structural internal parameters (u) and disorder constants (P). The calibrated energy gap of ZnO materials using FullBand simulator and Experimental band gap are also included for comparison.

DFT Methods	LDA	PBE	HSE06	LDA+U	Experimental	This Work
a (Å)	3.210[3]	3.284[4.5]	3.262[4.5]	3.197[6]	3.253[19-21]	**3.254**
c (Å)	5.136[3]	5.296[4.5]	5.212[4.5]	5.154[6]	5.205[19-21]	**5.21**
u	0.380	0.378	0.381	0.378	0.380	**0.380**
P*	0.000	0.002	-0.001	0.002	0.000	**0.000**
Eg (eV)	**0.7941**[3]	**3.413**[4.5]	**2.464**[4.5]	**1.1541**[6]	**3.44**[3-5]	**3.428**

* Journal of Electronic Materials (accepted for Publication).

ZnO: Full Band Simulator

ZnO Samples	t_{DS} (nm)			t_{WH} (nm)	Strain	Lattice Constant		Internal Parameter	Bond Length (Å)	Optical Band gap (eV)	Simulated Band gap (eV)
	(100)	(002)	(101)			a (Å)	c (Å)	u(P)			
Undoped	11	18	10	26	6.5×10^{-3}	3.246	5.238	0.398	2.013	3.22	**3.22**
0.45at.% **Cd**	16	20	17	13	-8.0×10^{-3}	3.328	5.190	0.4023	2.009	3.20	**3.19**
0.51at.% **Cd**	19	21	19	26	1.5×10^{-3}	3.332	5.161	0.4025	2.007	3.19	**3.22**
0.56at.% **Cd**	11	18	10	31	10.0×10^{-3}	3.313	5.225	0.4040	2.006	3.15	**3.15**
1at.% **Sr**	14	10	17	7.48	-1.64×10^{-2}	3.256	5.194	0.389	1.978	3.25	**3.27**
2at.% **Sr**	21	9	16	10.27	4.27×10^{-2}	3.251	5.194	0.389	1.976	3.26	**3.26**
3at.% **Sr**	9	6	6	4.14	9.95×10^{-2}	3.271	5.223	0.389	1.988	3.28	**3.33**
1at.% **Fe**	5	8	9	1.43	-14.8×10^{-2}	3.236	5.194	0.380	1.967	3.24	**3.26**
2at.% **Fe**	3	5	7	0.65	-34.5×10^{-2}	3.231	5.194	0.380	1.968	3.26	**3.25**
3at.% **Fe**	8	5	7	9.06	6.6×10^{-2}	3.231	5.186	0.380	1.970	3.29	**3.25**

Undoped, Cd, Sr and Fe doped ZnO thin films (Sol gel) along with optical and simulated energy band gaps

* Journal of Electronic Materials (accepted for Publication).

Group-III Nitrides: Full Band Simulator

Energy difference obtained using FullBand simulator based on the proposed model compared with those reported earlier, with those computed from reported various density functional theory (DFT) techniques and with experimental results

Material	Previously reported values of E_g	E^{LDA}	$E^{LDA-1/2}$	DFT^{PBE}	DFT^{HSE}	Experiments	$E^{This\ work}$
AlN	6.54[7], 6.23[10]	4.50[5,7]	6.06[5]	4.13[7], 4.02[20]	6.42[7], 6.29[20]	6.23[5], 6.026[17], 6.1-6.2[7,20]	**6.20**
GaN	3.5[7], 3.507[10]	2.02[5], 2.11[7]	3.52[5]	1.69[7,20]	3.55[7,] 3.55[20]	3.507[5], 3.35[22], 3.51[20]	**3.47**
InN	0.7–1.0[7,8], 0.7-1.9[10]	-0.03[5], -0.24[7]	0.95[5]	− 0.42[7,20]	0.86[7], 0.86[20]	0.7-1.9[5], 0.6-0.7[20]	**0.7**
$Al_{0.2}Ga_{0.8}N$	3.99*	2.353[5]	3.951[5]	4.570[12]	4.569[12]	3.962[24]	**3.94**
$In_{0.2}Ga_{0.8}N$	2.72-2.78*	1.52[5]	2.76[5]	2.272[5]	1.925[12]	2.625[23]	**2.66**
$In_{0.2}Al_{0.8}N$	4.7 - 4.76*	3.431[5]	4.409[5]	3.445[12]	2.976[12]	4.515[25]	**4.71**

* Scientific Reports, Nature **Journal (under Review).**

MOBILITY CHARACTERIZATION

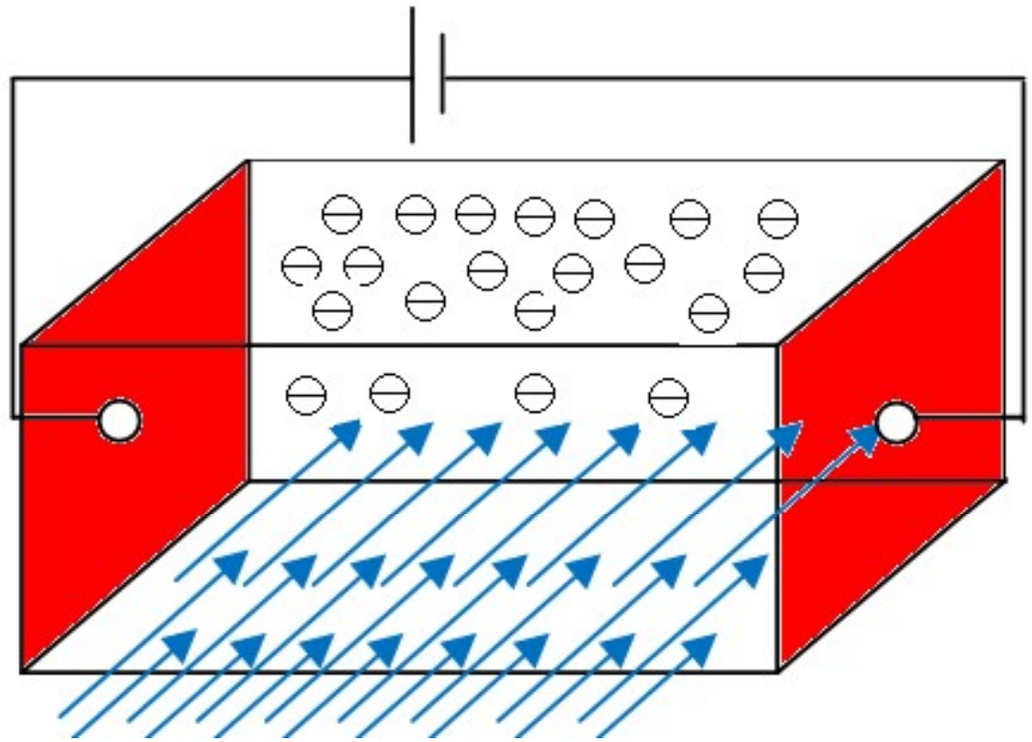

MATERIAL CHARACTERIZATION

Free Electrons

❑ **For free particles, the electron wave function is the solution to the time-independent Schrödinger equation:**

$$\left(\frac{\hbar^2}{2m}\nabla^2 + E\right)\emptyset(r) = 0$$

❑ **The solutions form the basis of plane waves:**

$$\emptyset_k(r) = C_k e^{ik.r} \qquad \textbf{with} \qquad k^2 = k_x^2 + k_y^2 + k_z^2 = \frac{2mE}{\hbar^2}$$

❑ The velocity, **v, of a particle represented by a wave packet** centered around the crystal momentum, **k, is obtained from** the *dispersion relation between* ***k and the energy E as***

$$E_k = \frac{\hbar^2 k^2}{2m} \ldots\ldots\ldots\ldots v = <\left|\frac{\hbar}{i}\nabla\right|> = \frac{1}{\hbar}\nabla_k E_k = \frac{\hbar k}{m} \qquad \text{and} \qquad D(E)dE = \frac{2m^{3/2}E^{1/2}}{\sqrt{2}\pi^2\hbar^3}dE$$

ELECMOB SIMULATOR

Features

- ❑ Graphical User Interface (GUI) on Windows based application
- ❑ Boltzmann transport equation solution with Ensemble Monte Carlo Technique
- ❑ Include standard scattering mechanisms following Fermi Golden Rule for momentum & energy
- ❑ Modeled beyond the effective-mass approximation on the full electronic band structure obtained from FullBand Simulator
- ❑ The electron-phonon, electron-impurity, and electron-electron scattering rates included in a way consistent with the full band structure of the solid
- ❑ Accounting for density-of-states and matrix-element effects more accurately
- ❑ The carrier transport on the full energy band under influence of electromagnetic forces
- ❑ Accurate up to particle level

ELECMOB SIMULATOR

- The Boltzmann Transport Equation (BTE) is

$$\frac{df}{dt} + \nabla_k E(k).\nabla_r f + F.\nabla_p f = \left|\frac{df}{dt}\right|_{scattering} + GR$$

Here f is the distribution function, E is the electric field, F is the external electromagnetic force.

- Solution of 6+1 dimensional is possible through:
  - A spherical harmonic expansion (SHE) method with initial approximations
    - accuracy of simulation results ??
  - The ensemble Monte Carlo (EMC) technique (stochastic) is best suited to simulate non-equilibrium transport in semiconductor.
  - In Monte Carlo (MC) method, physics is more straightforward and provides flexibility in exploring physical mechanisms and carrier transport.

Scattering Mechanisms

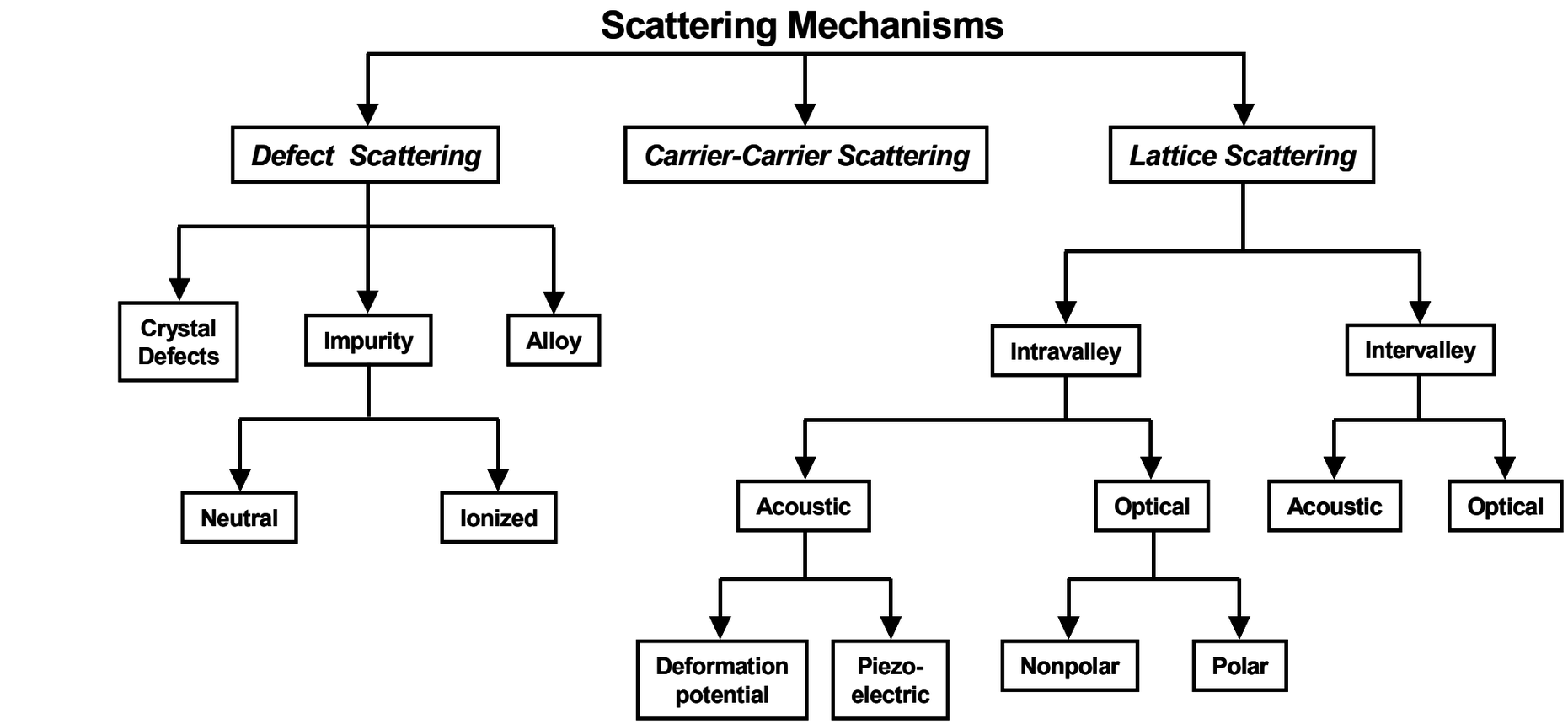

ELECMOB SIMULATOR

- **Under the influence of Electromagnetic forces the carrier:**

$$k(t) = k(0) - \frac{e(E + v \times B)t}{\hbar}$$

where

$$v = \frac{1}{\hbar}\frac{dE}{dk} \quad \& \quad \frac{\partial k}{\partial t} = \frac{qE}{\hbar}.$$

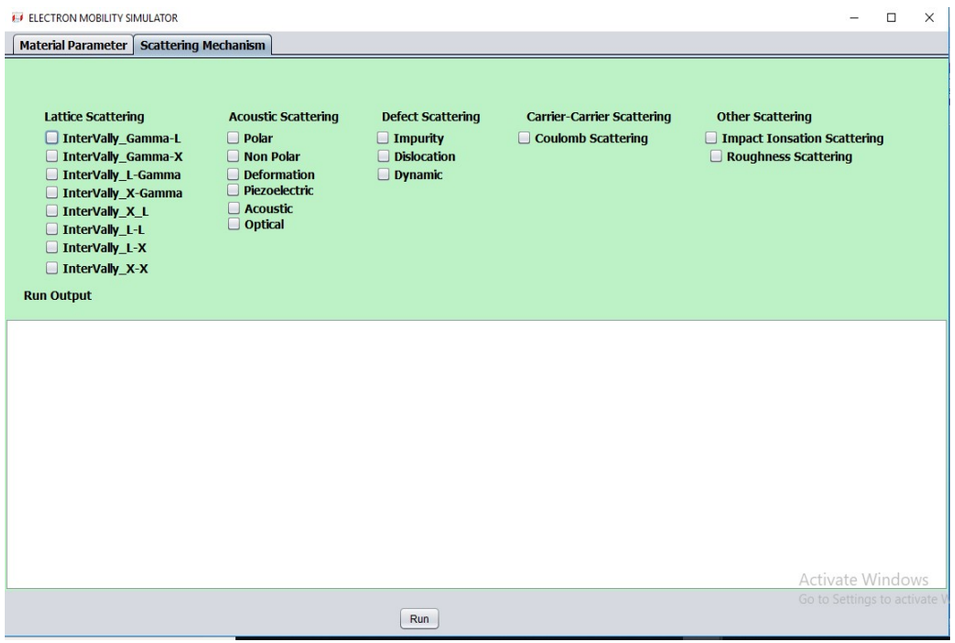

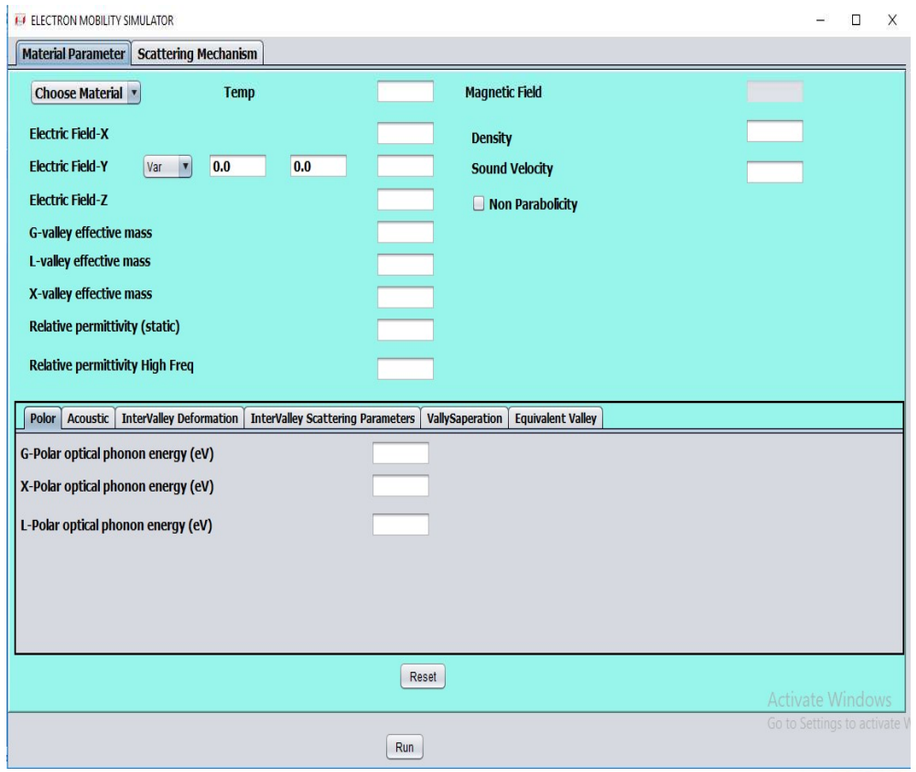

GROUP-III NITRIDES

The Comparison of simulated electron drift velocity as a function of applied electric field with the reported literature. Data from present work is displayed as solid lines where as experimental/theoretical results are depicted by open circles, squares and triangles for AlN, GaN and InN respectively.

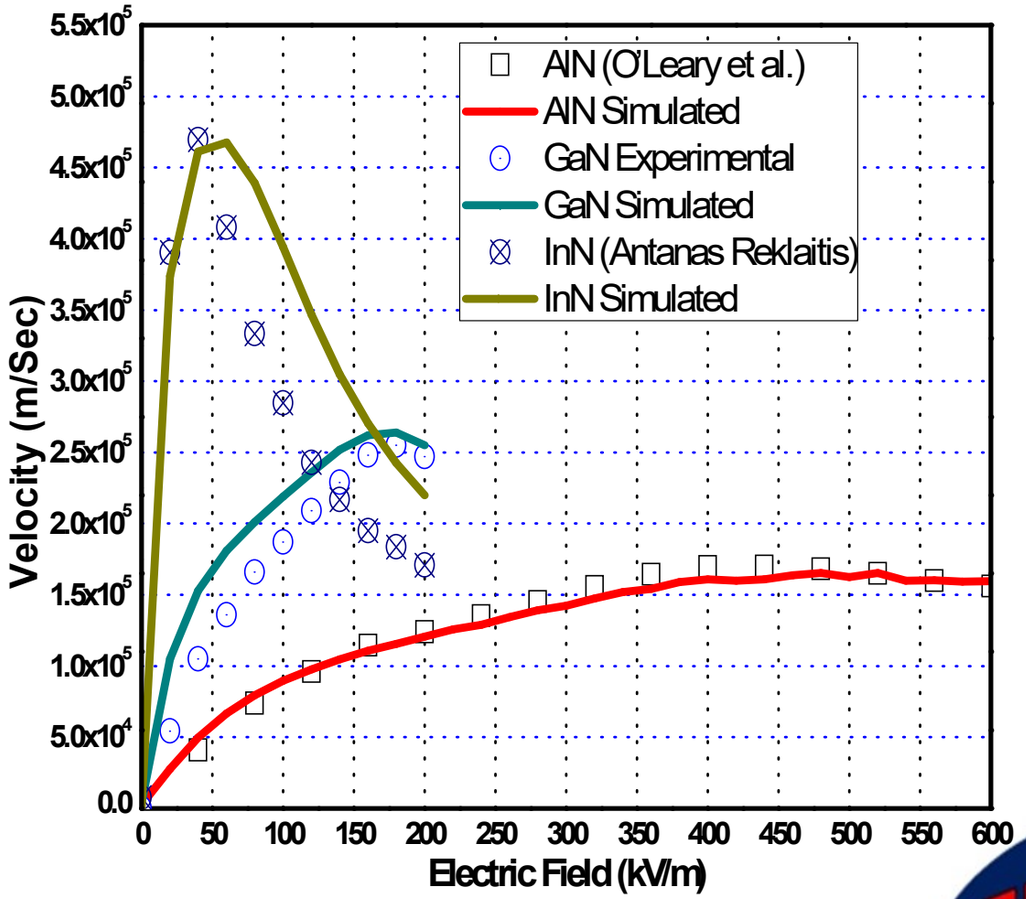

❖Anshika Srivastava, Anshu Saxena, Praveen K. Saxena, F. K.Gupta, Priyanka Shakya, *at. el*., An innovative technique for electronic transport model of group-III nitrides, ***Scientific Reports nature research*** (2020) **10**:18706.

SCATTERING RATES

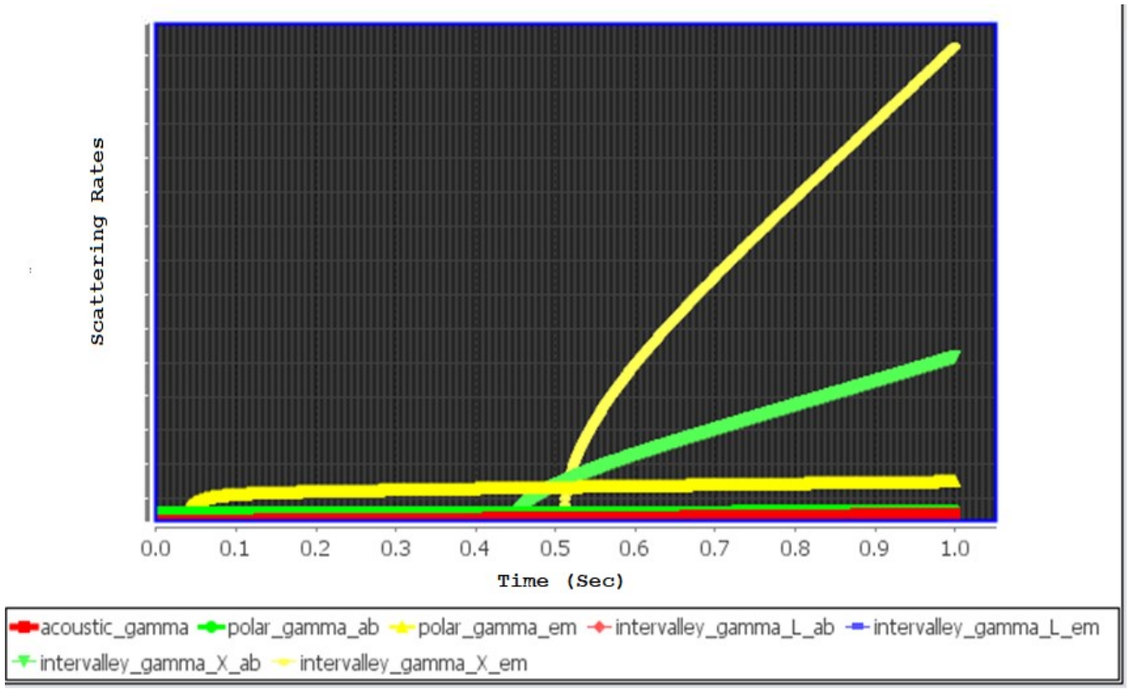

Γ- Valley

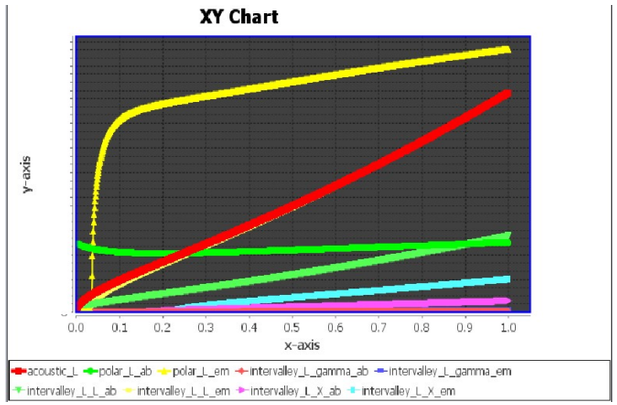

U- Valley

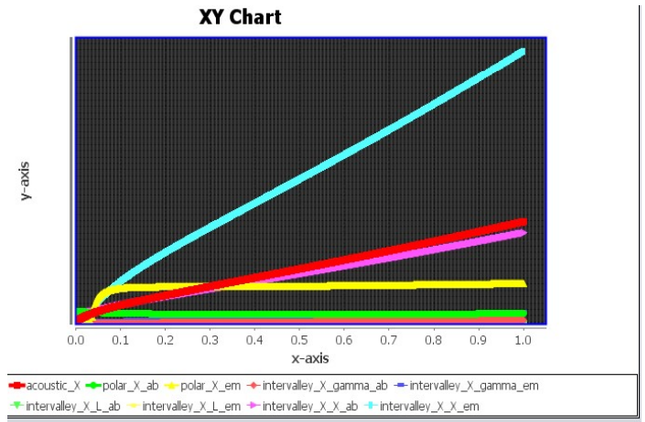

Γ_3- Valley

OCCUPATION

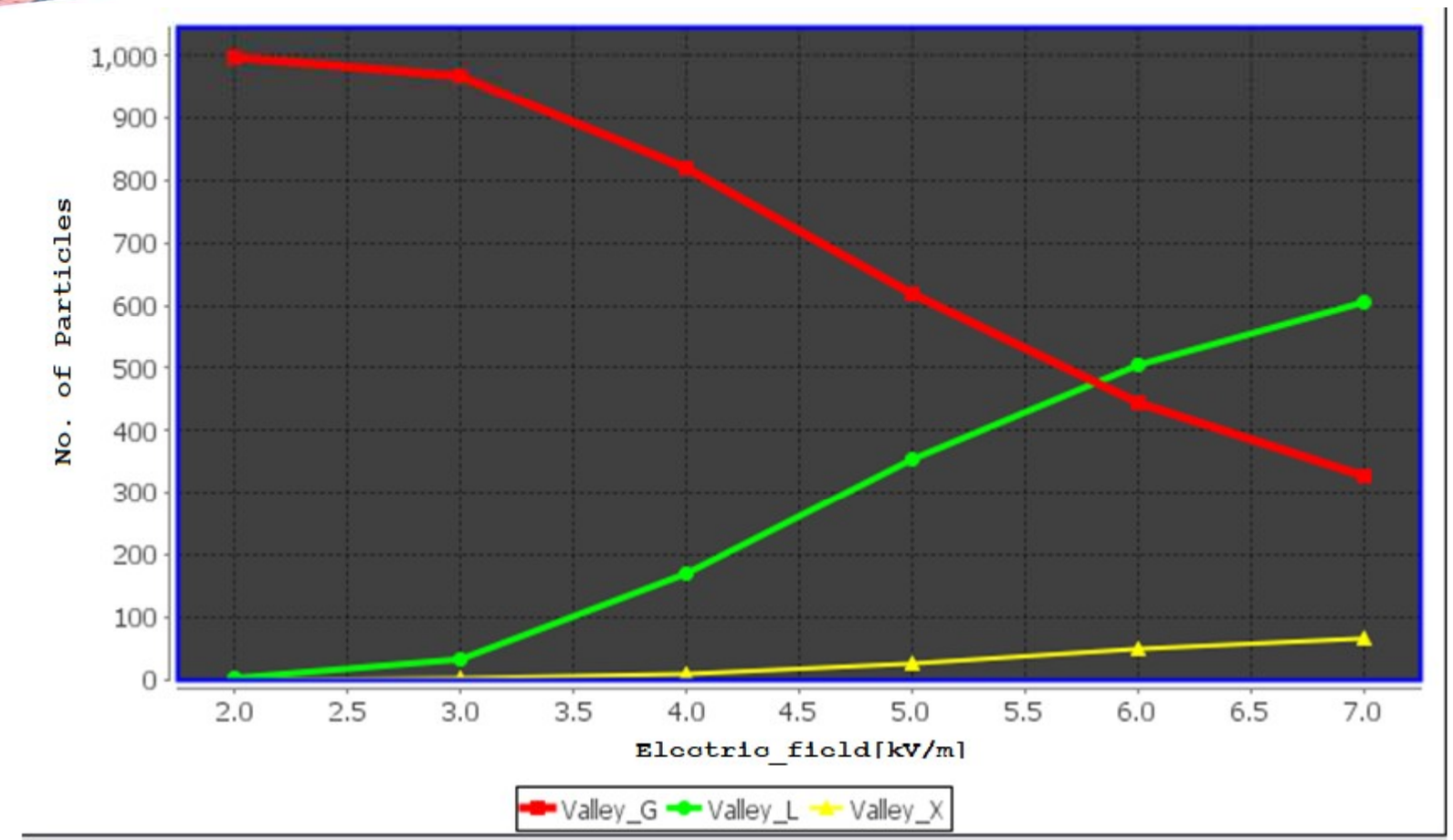
No. of Particles
1,000
900
800
700
600
500
400
300
200
100
0
2.0
2.5
3.0
3.5
4.0
4.5
5.0
5.5
6.0
6.5
7.0
Electric_field[kV/m]
Valley_G
Valley_L
Valley_X

MOBILITIES

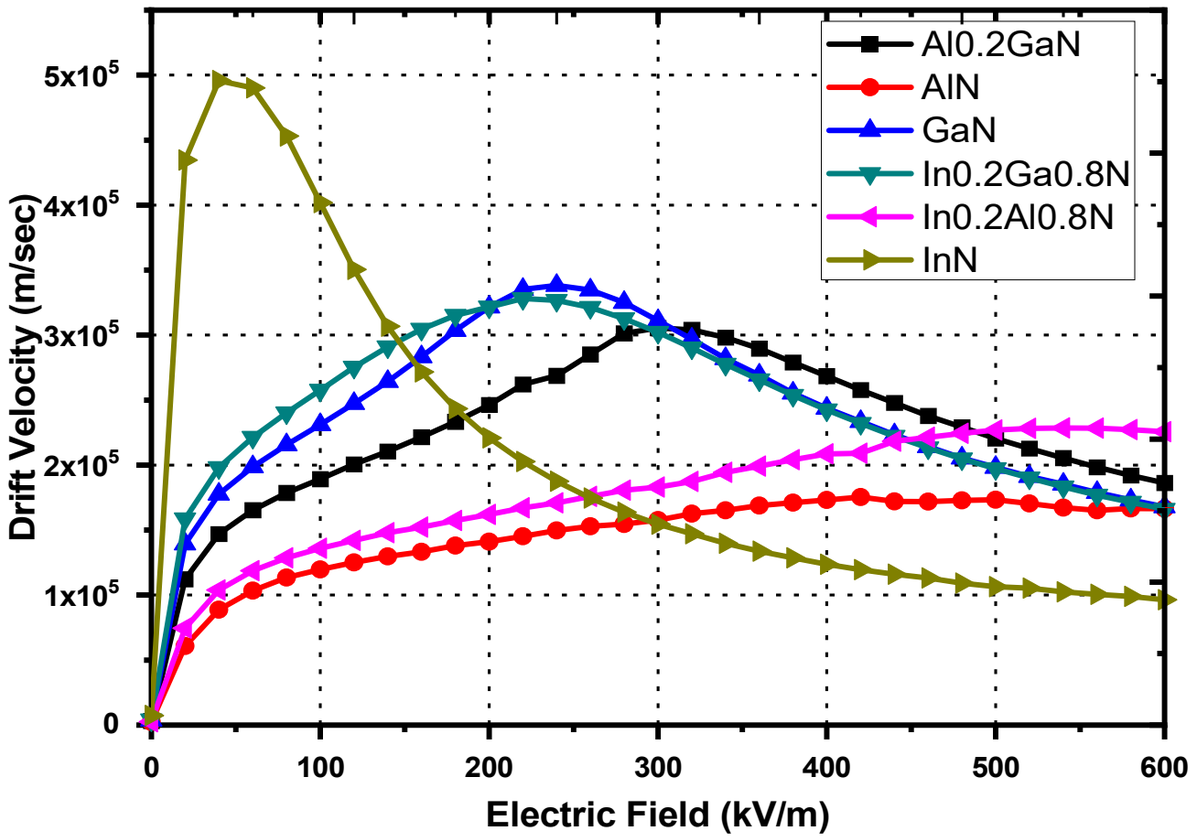

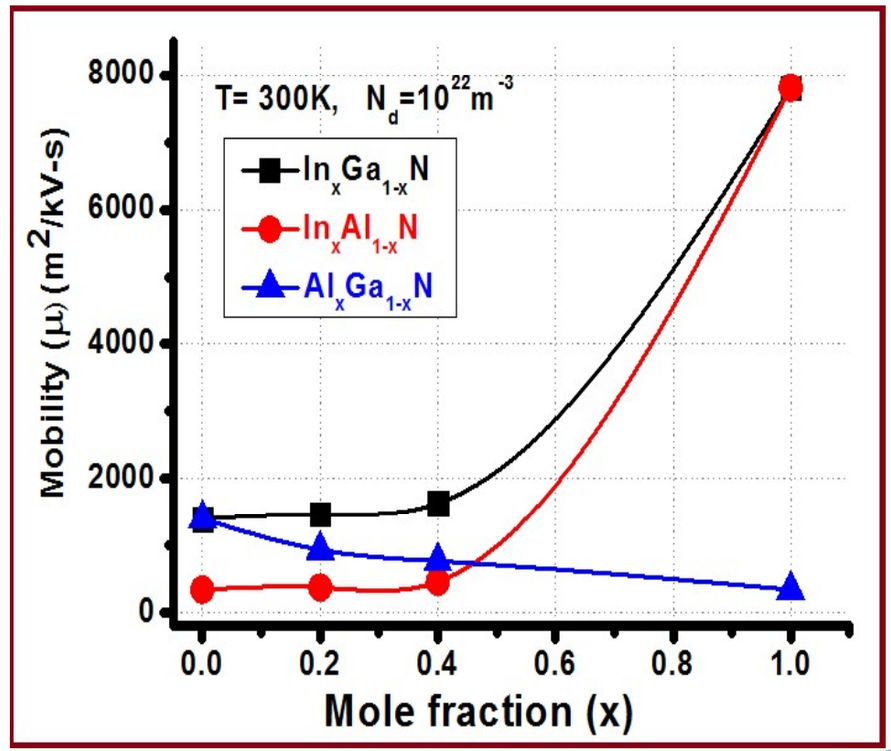

* Scientific Reports, Nature **Journal**.

Temp Effect On Mobilities

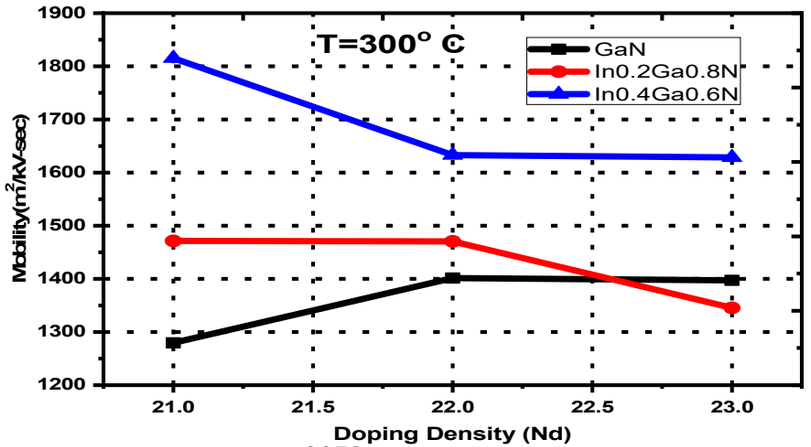

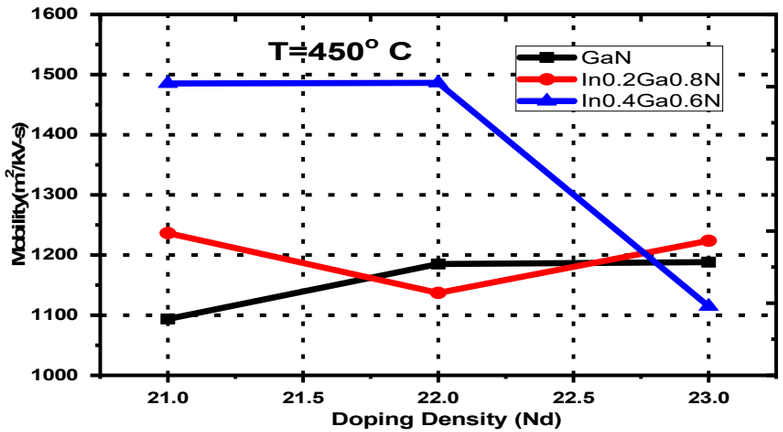

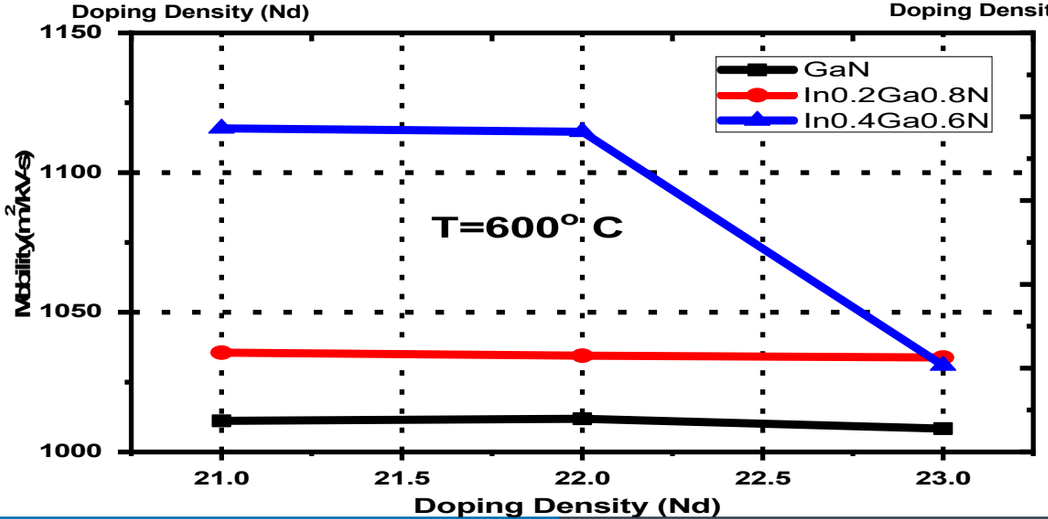

Mobilities Ternary Compounds

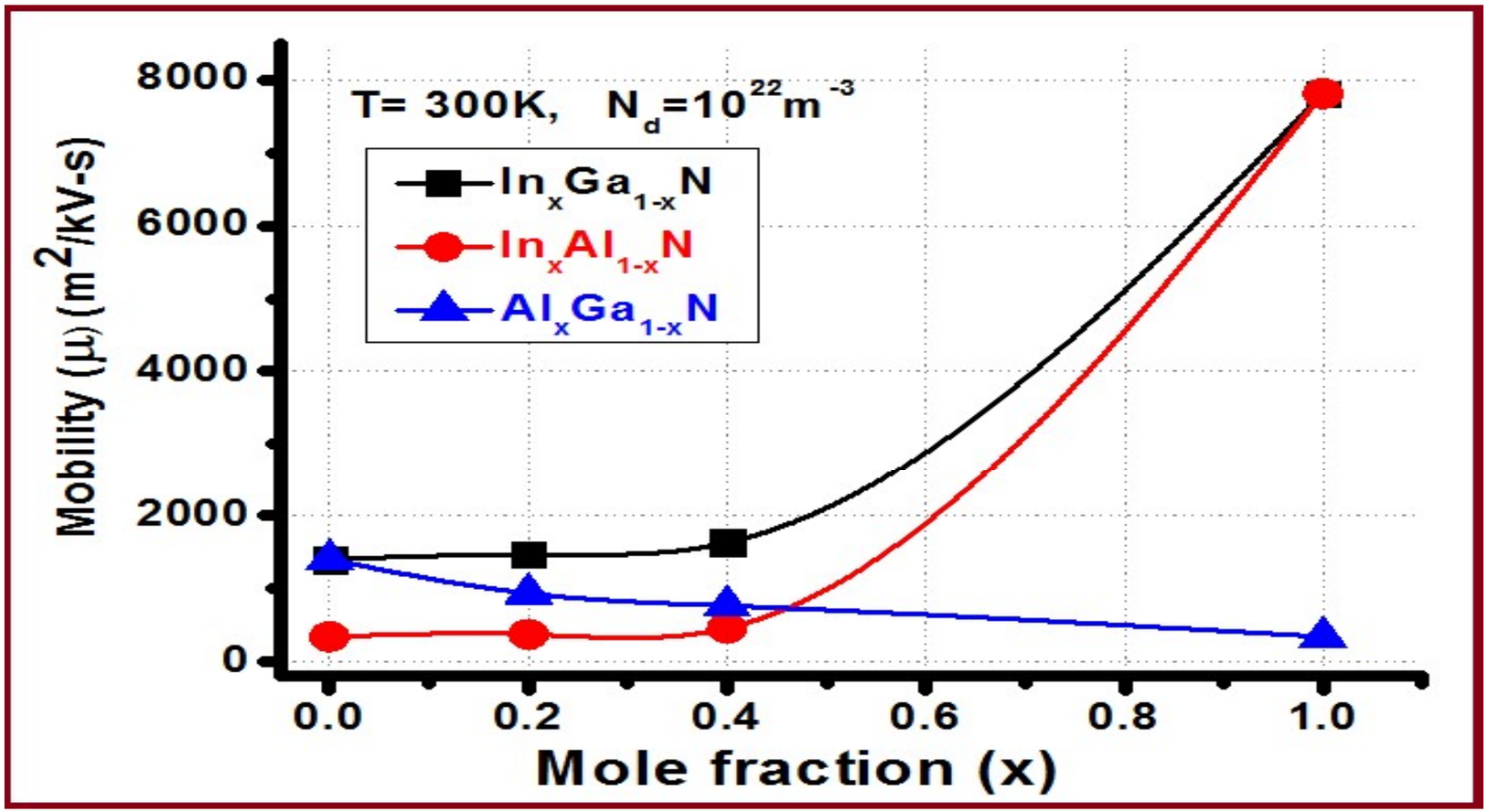

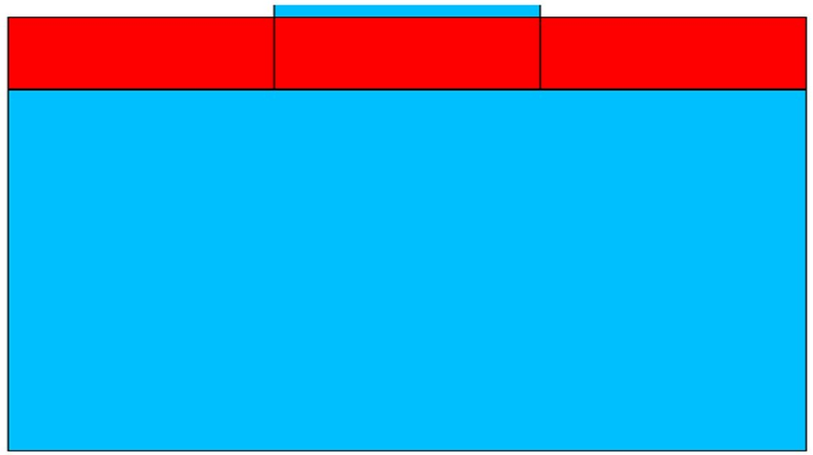

Monte Carlo Particle Device Simulator

Technology of Next Level
driven through innovation

DEVICE MODELING

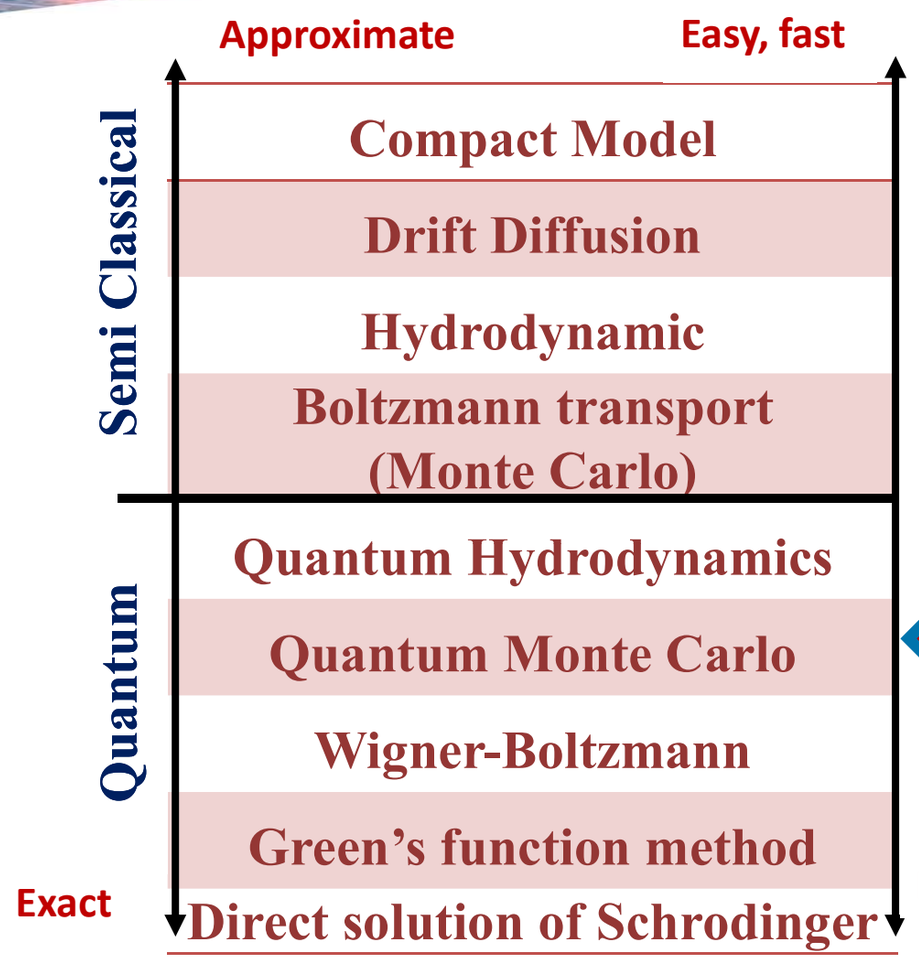

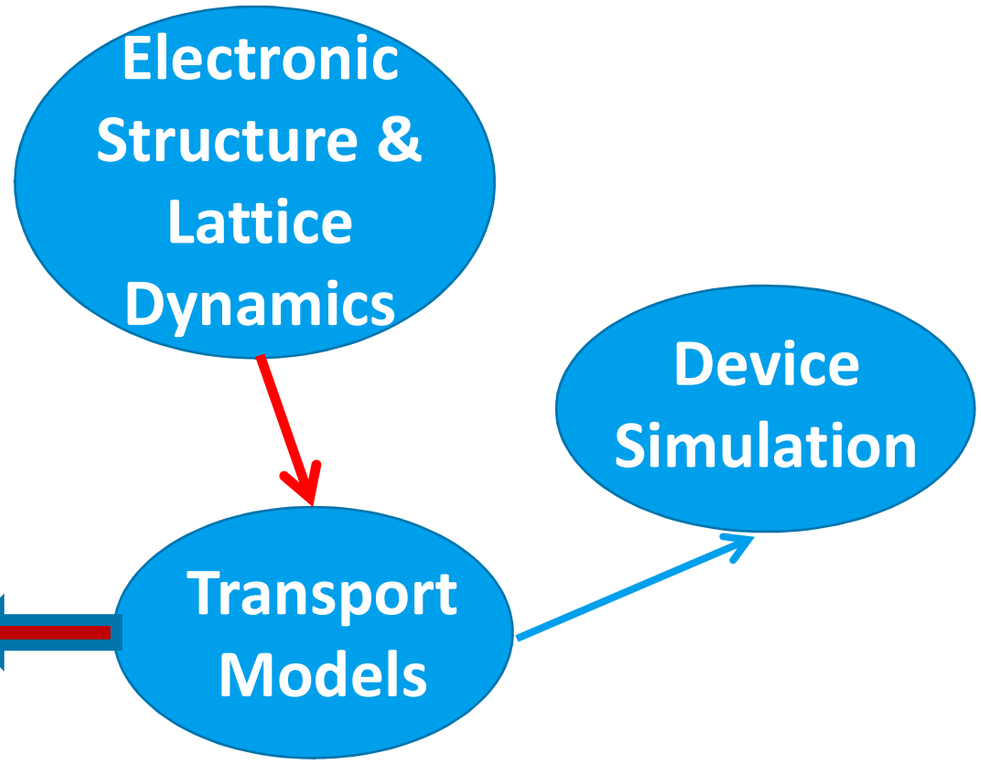

PARTICLE DEVICE SIMULATOR

- Particle device simulator takes into account the transport of Monte Carlo particles (Super particles).
- Under influence of applied field, determined self-consistently through the solution of decoupled Poisson's and BTE equation over a suitably small time-step.
- The time step is taken typically less than the inverse plasma frequency obtained with the highest carrier density in the device.

FLOW CHART

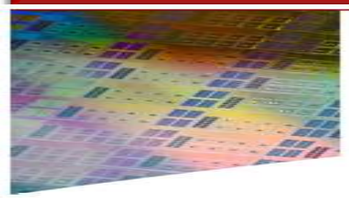




Flow Chart for program implementation

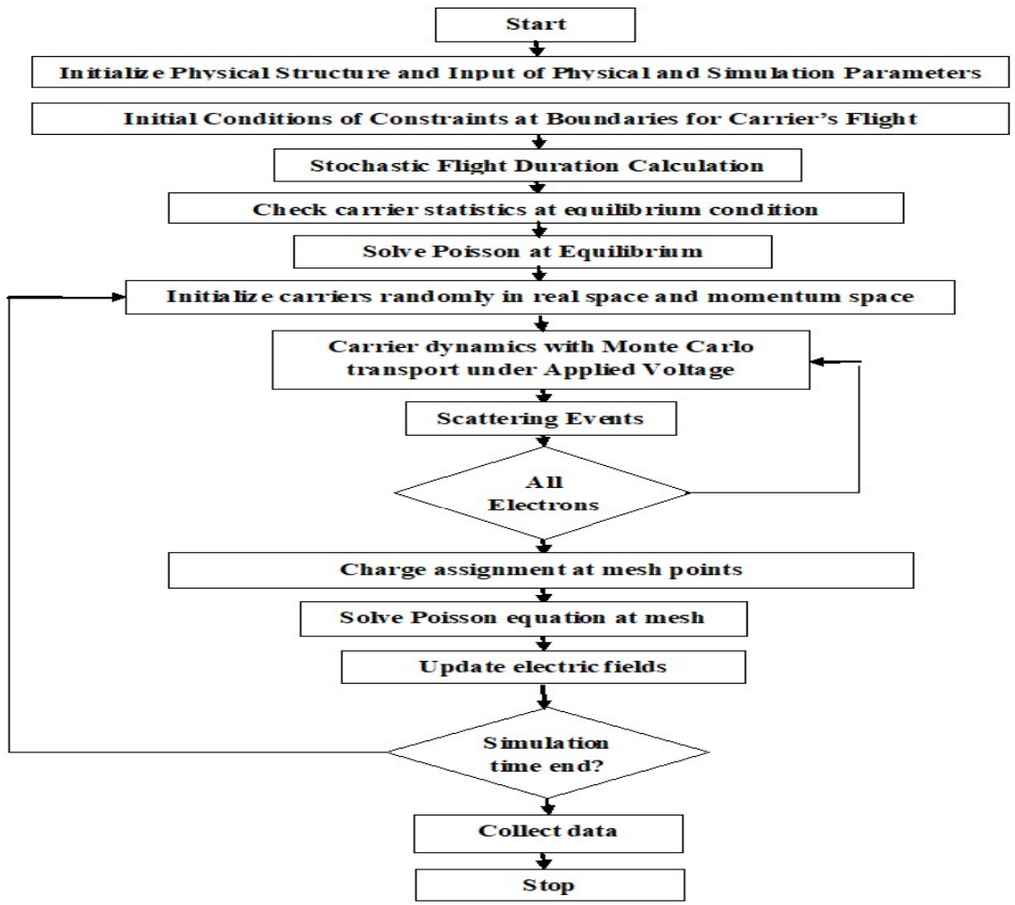

PARTICLE DEVICE SIMULATOR

Technologies implemented in Monte Carlo Particle Device Simulator:

- **MOSFET**
- **FDSOI**
- **Tunneling FET**
- **MESFET**
- **HEMT**

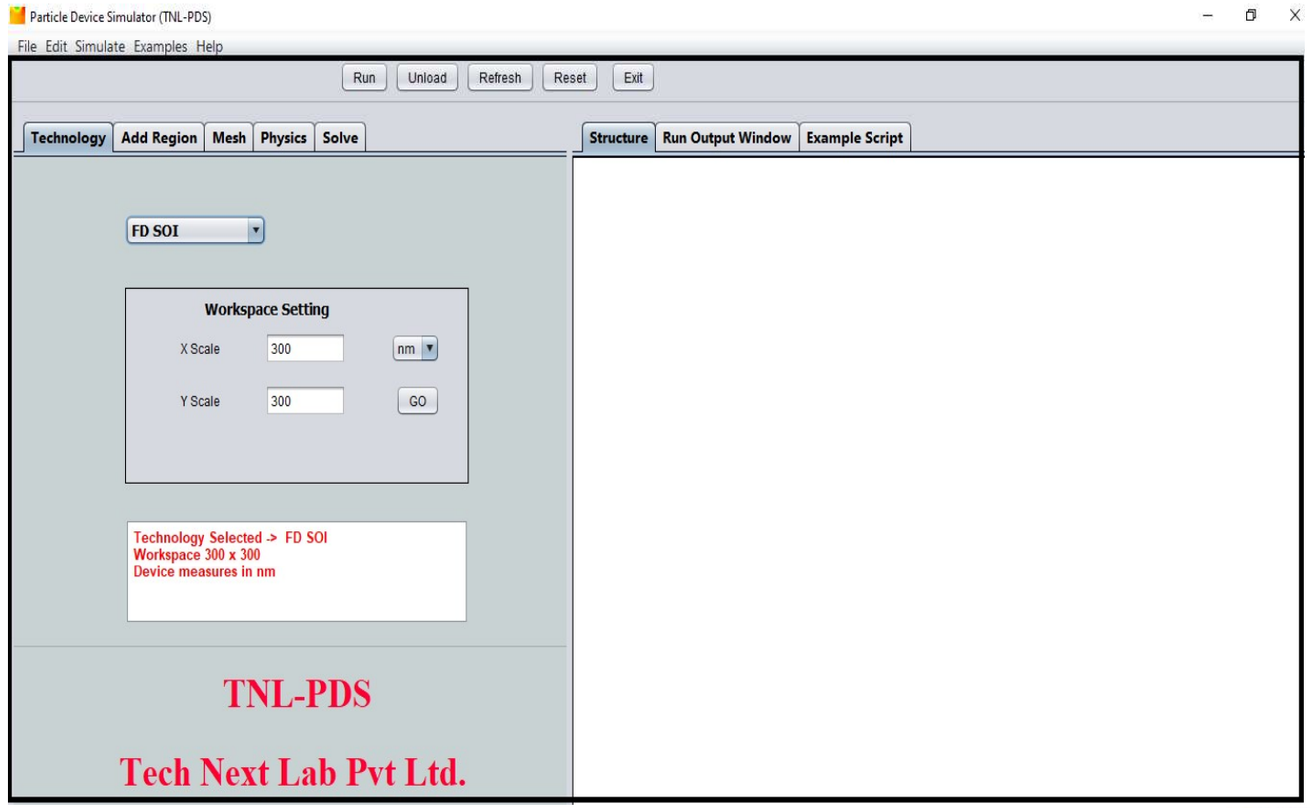

PARTICLE DEVICE SIMULATOR

- Poisson’s solution generated over the node points of the mesh,
- Carrier transport solution is obtained using Ensemble Monte Carlo (EMC) on the full range of space coordinates in accordance with the particle distribution itself.
- Particle-mesh (PM) coupling scheme is used for assignment of carrier charge on different nodes and for calculation force on each charges.

SOLUTION

- The classification of Particle-mesh (PM) coupling scheme is included as;
  - Carrier charge assign at mesh nodes Charge in Cloud (CIC) scheme,
  - Solution of Poisson's equation on node points through Successive over Relaxation (SOR) method,
  - Calculation of the mesh defined electric field components,
  - Interpolation of forces at the particle positions.

BOUNDARY CONDITIONS

- Particle Device Simulator (PDS) contains consistent boundary conditions with those imposed on the potential on the field.
- The particle boundary conditions contain Neumann (zero electric field in the direction normal to the surface) and Dirichlet (contacts) conditions.
- At Neumann boundary the reflecting boundaries has been taken.

QUANTUM CONFINEMENT EFFECT

- Density-gradient model: implemented dependent on non-local quantities.
- Density gradient model is first-order quantum-correction model describe carrier confinement by locally modifying the electrostatic potential through a correction potential γ.
- The Boltzmann-Wigner transport equation can be derived as

$$\frac{\partial f}{\partial t} + v.\nabla_r f - \frac{q}{\hbar}\sum_{\alpha=0}^{\omega}\frac{(-1)^{2\alpha}}{4^{\alpha}(2n+1)!}\nabla_k^{2n+1}V(r).\nabla_k^{2n+1}f = \left(\frac{\partial f}{\partial t}\right)_{coll}$$

QUANTUM CONFINEMENT EFFECT

- The corrected quantum effect is included as

$$\frac{\partial f}{\partial t} + \frac{\hbar . k}{m^*} \nabla_r f - \frac{1}{\hbar} \nabla_r \left(V(r) - \nabla_r^2 \emptyset \right) \nabla_k f = \left(\frac{\partial f}{\partial t} \right)_{coll}$$

The correction potential term in multidimensional space is

$$\gamma(r,t) = \frac{\hbar^2}{12 \lambda k_b T m^*} \left(\nabla_r^2 \emptyset(r,t) - \frac{1}{2 k_b T} \left(\nabla_r \emptyset(r,t) \right)^2 \right)$$

The fitting parameter λ is determined by comparing the carrier density in a device structure to the carrier density obtained by the solution of Poisson Equation.

PARTICLE MESH COUPLING

- The particle-mesh method is a widespread model for space charge calculations.
- Particle dynamics under applied electric field requires accurate solution of Poisson's equation.
- The particle simulation means the assignation of the particle's charge to the rectangular mesh.
- Two types of the most famous particle-mesh (PM) coupling schemes:
  - Nearest Grid Point (NGP)
  - Cloud In Cell (CIC)
  - (NEC)

Case Studies

GaNFET Simulation

*P. K. Saxena *at. el.,* Atomistic Level Process to Device Simulation of GaNFET Using TNL TCAD Tools, Book Chapter, © ***Springer Nature*** (2020) 176, Lecture Notes in Electrical Engineering ISBN 978-981-15-5261-8 ISBN 978-981-15-5262-5 (eBook)

GaNFET Epitaxial Growth

Epi-growth has been done with the following process parameters:

Parameters	Values	Unit
Time	30	s
Temperature	800	°C
Surface energy	2	eV
Desorption barrier energy	4	eV
Schwoebel barrier	0.002	eV
Incorporation barrier	0.05	eV
Nearest neighbor attraction	0.05	eV

Precursors and gas ambience used during simulation

Materials	Partial pressure		
	Ga (mbar)	Al (mbar)	N2 (mbar)
GaN	0.3	0.0	3.0
$Ga_{0.85}Al_{0.15}N$	0.3	0.03	3.0
$Ga_{0.7}Al_{0.3}N$	0.28	0.05	3.0
$Ga_{0.61}Al_{0.39}N$	0.25	0.10	3.0

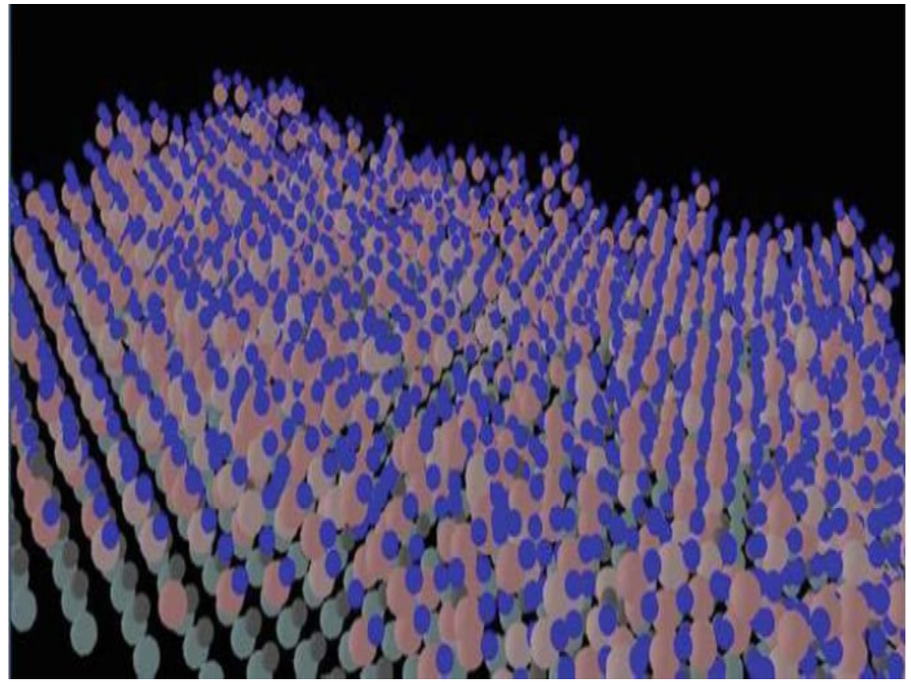

GaNFET Case Studies

Variation of lattice constant with Al mole fraction

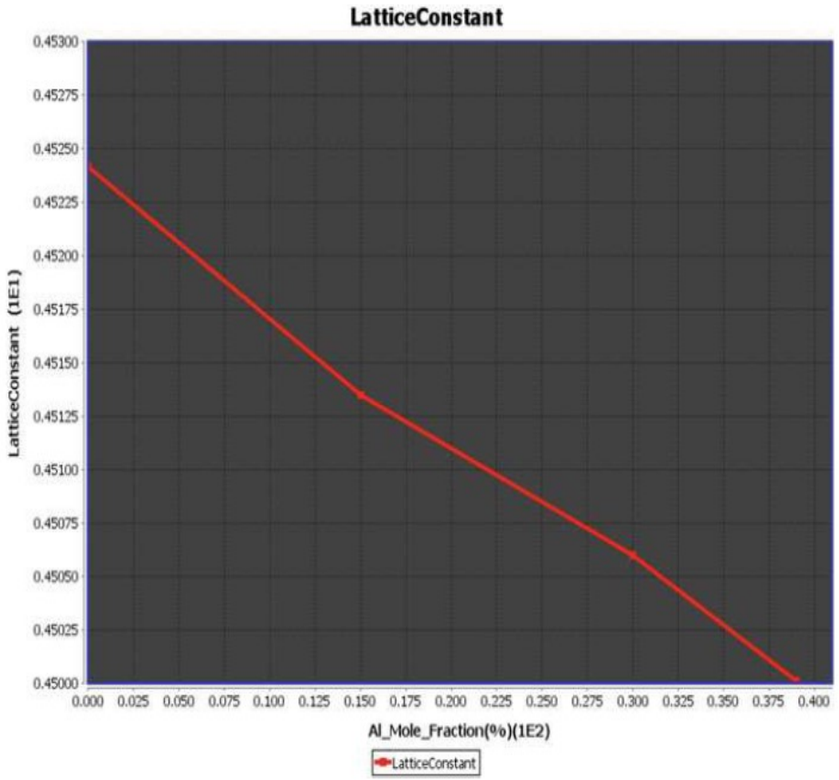

Surface roughness at the interface of AlGaN/GaN

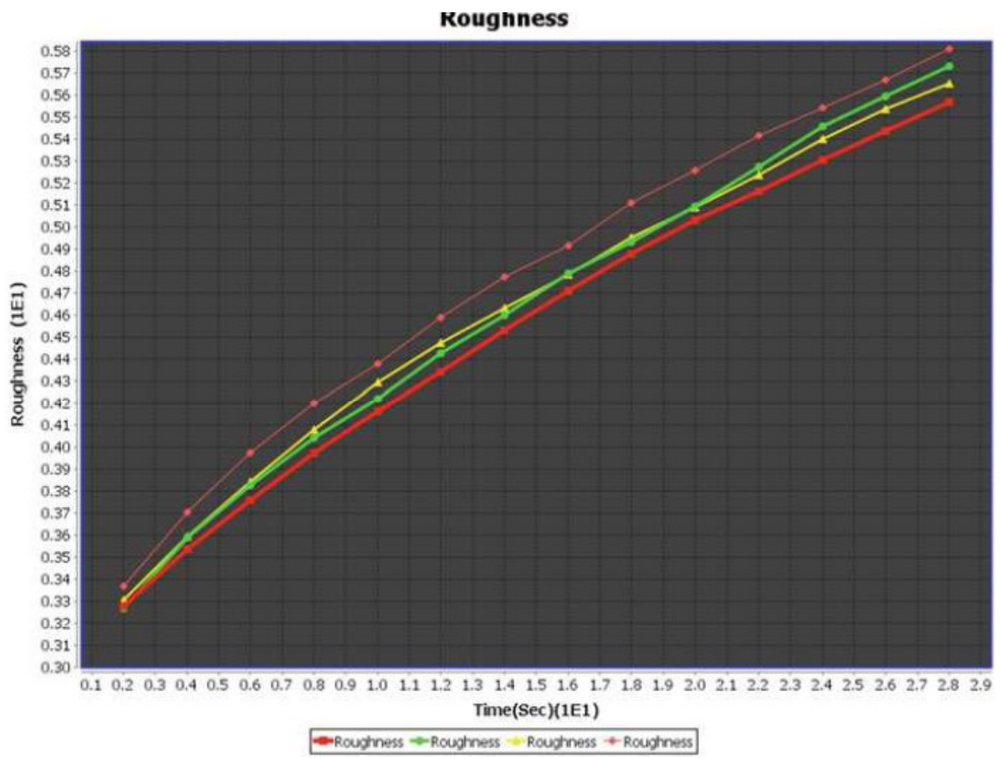

GaNFET Case Studies

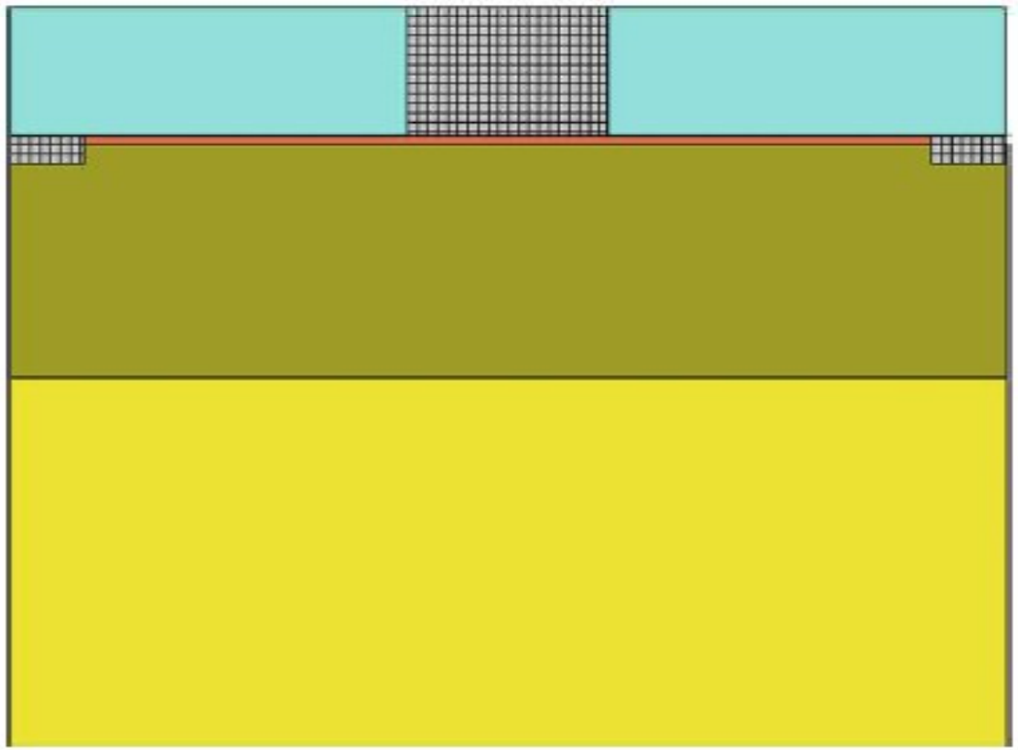

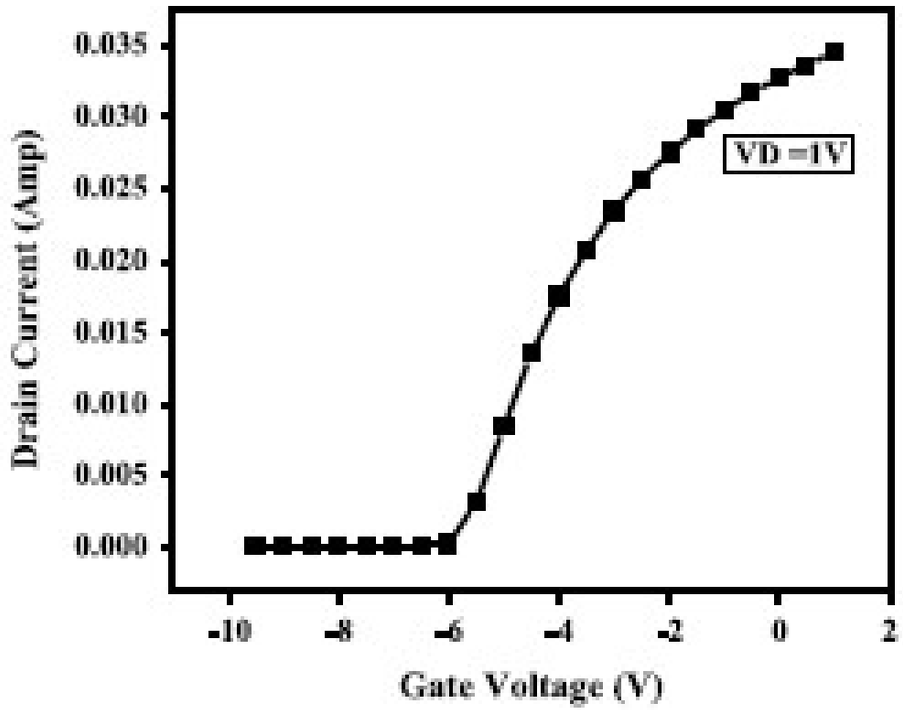

Fig. 9 Device structure with 25 nm thick AlGaN/GaN layer grown on SiC (100) substrate

GaNFET Case Studies

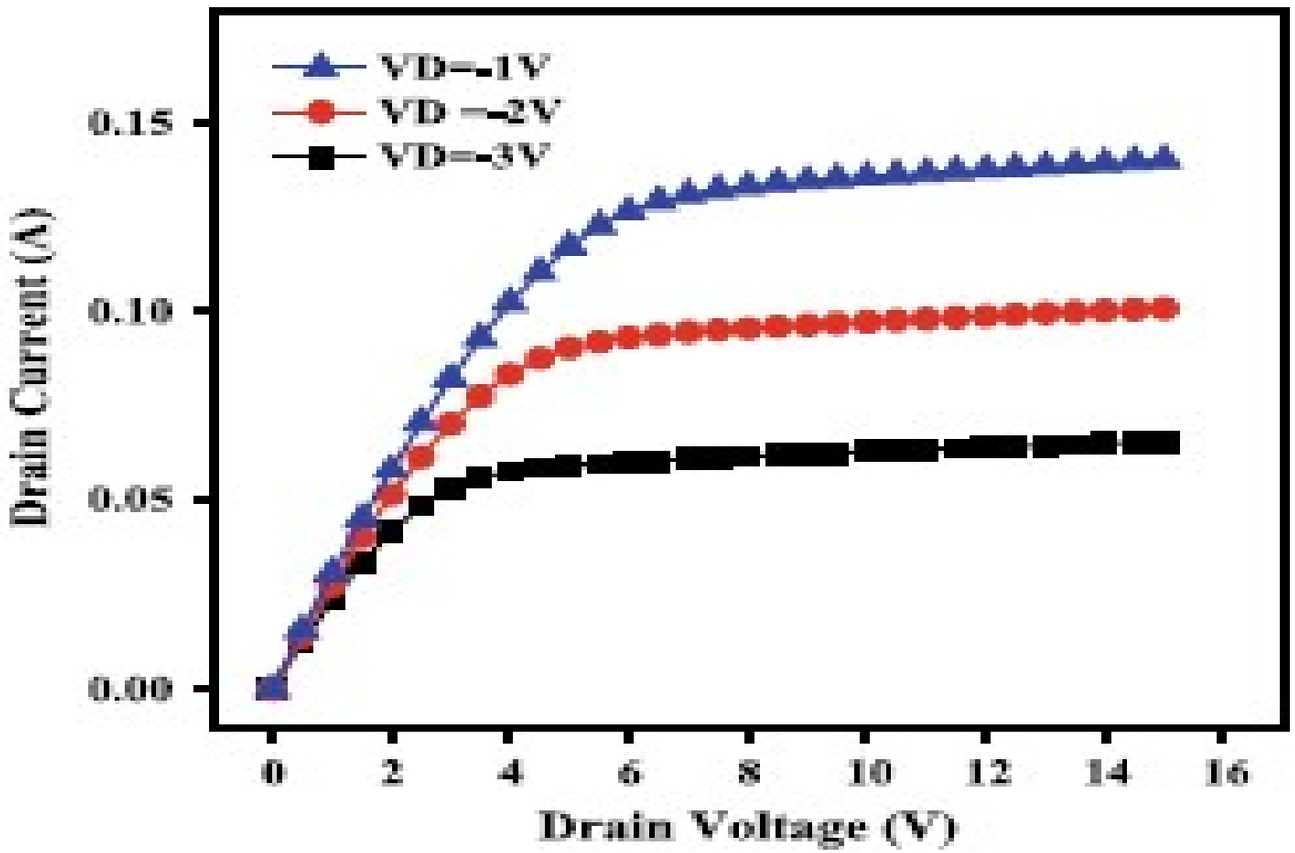

Optical Device

InGaAs/InP Infrared Photodetector

*P. K. Saxena *at. el.,* Numerical simulation of InxGa1−xAs/InP PIN photodetector for optimum performance at 298 K, *Optical and Quantum Electronics* (2020) **52**:374

Infrared Detector

p^+- $In_{0.53}Ga_{0.47}As$ (150 nm)	p- InP	*i*- $In_{0.53}Ga_{0.47}As$ (2.5µm)	n-InP (2.6 µm)

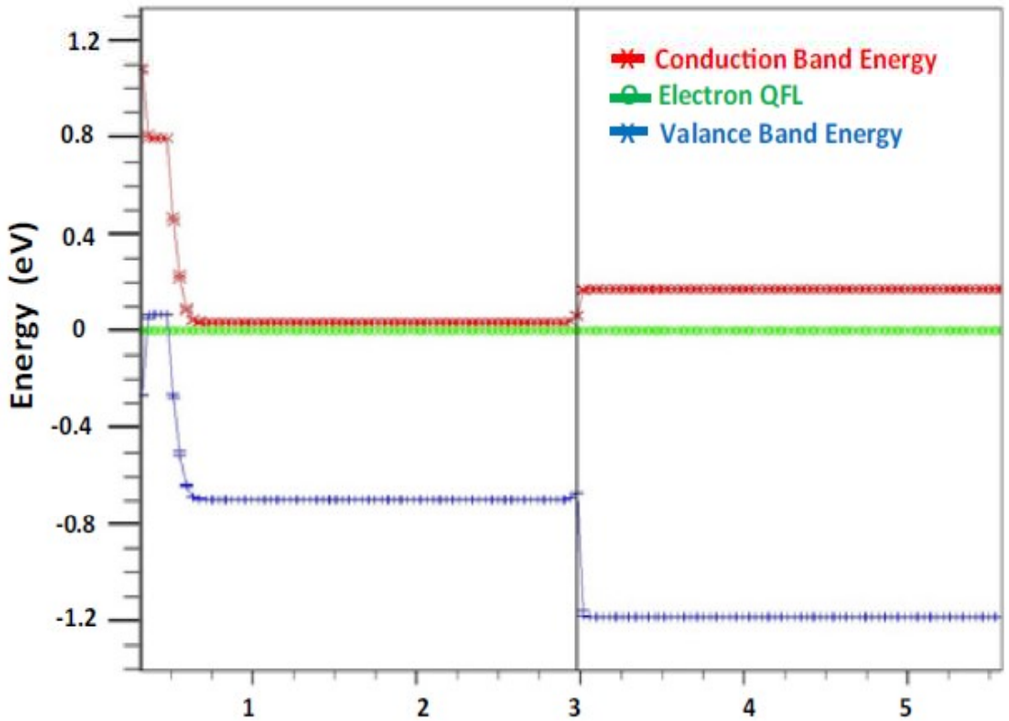

I – V Characteristics

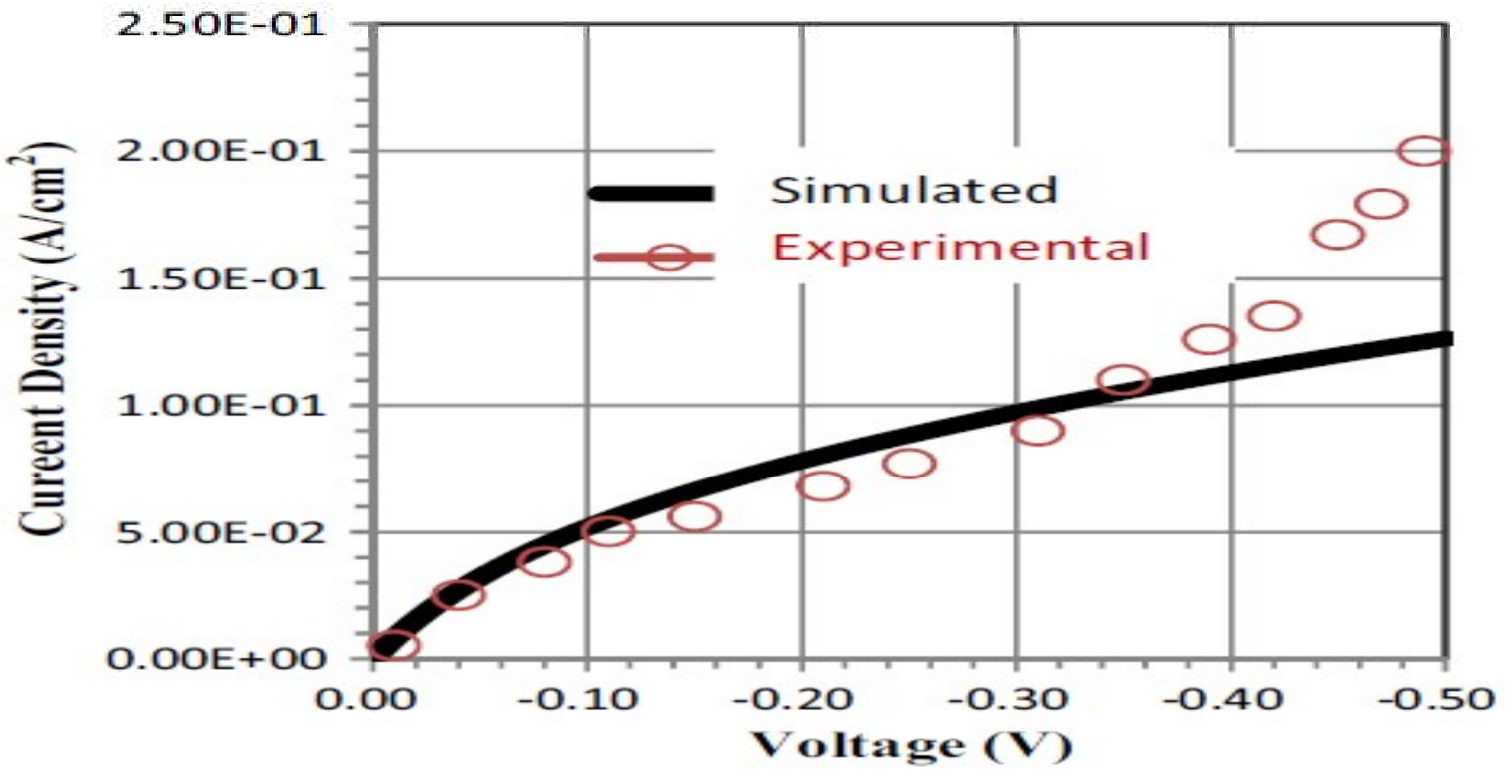

Infrared Detector

Table 1 The current density values for different doping dose at specified absorbing layer thickness

Doping dose (cm^{-3})	Current density at specified absorbing layer thickness (A/cm^2)		
	2 μm	2.5 μm	3 μm
5.1×10^{15}	2.53×10^{-07}	2.53926×10^{-07}	2.54×10^{-07}
1.1×10^{16}	1.62×10^{-07}	1.63×10^{-07}	1.63×10^{-07}
5.1×10^{16}	2.6456×10^{-08}	2.6898×10^{-08}	2.7595×10^{-08}

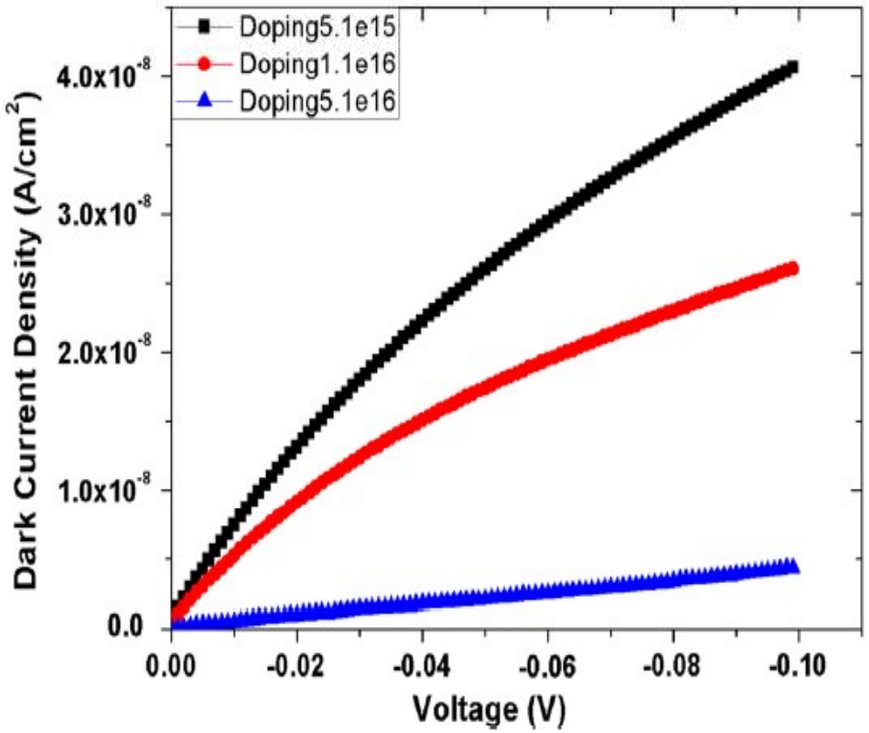

Quantum Efficiency

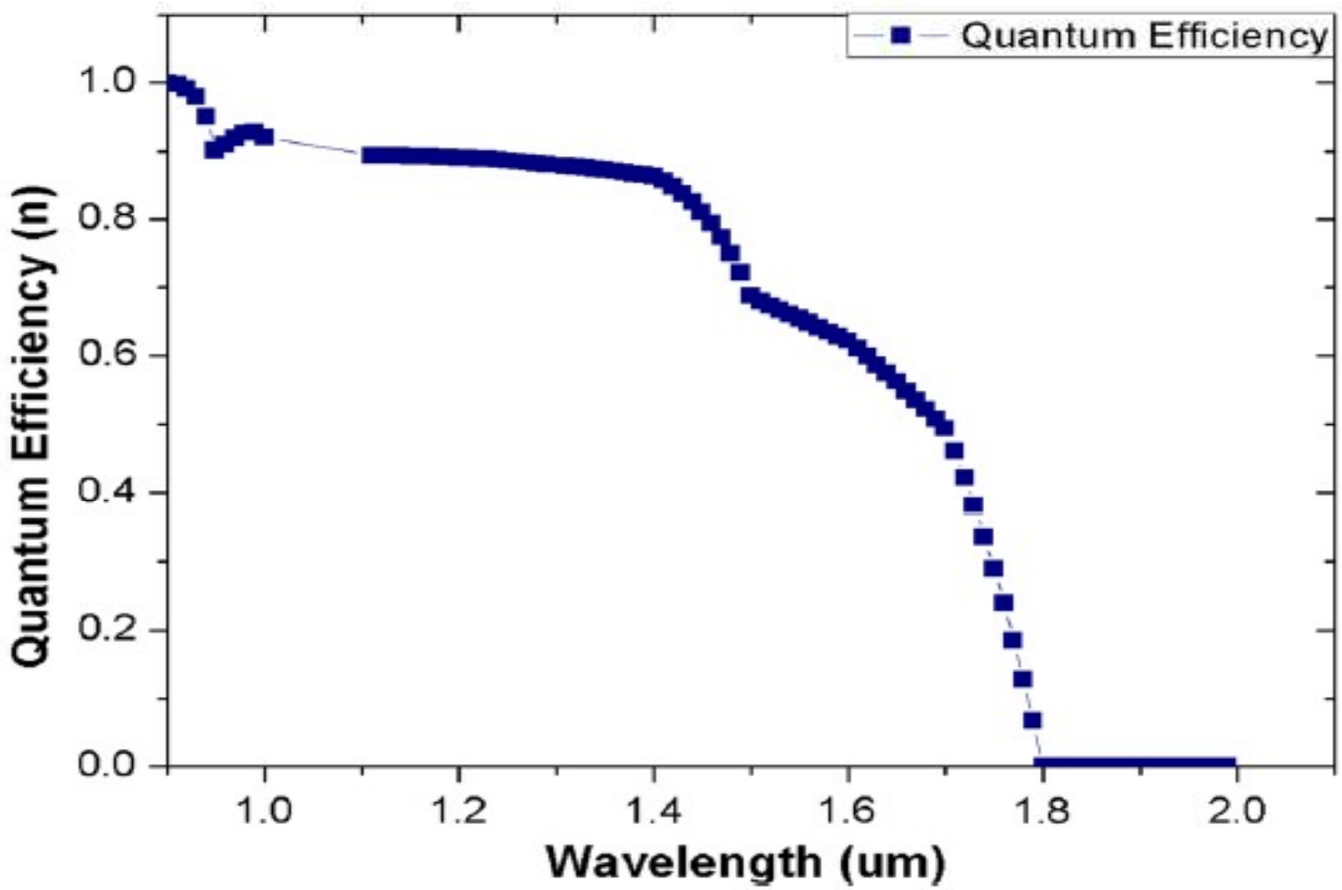

Infrared Detector

FDSOI MOSFET

FDSOI MOSFET

*P. K. Saxena *at. el.,* A Comparative Study for Scaling FDSOI Technology up to 7nm –Based on Particle device Simulation, *Jaournal of Nano & Optoelectronics*(2020), under Review.

FDSOI MOSFET

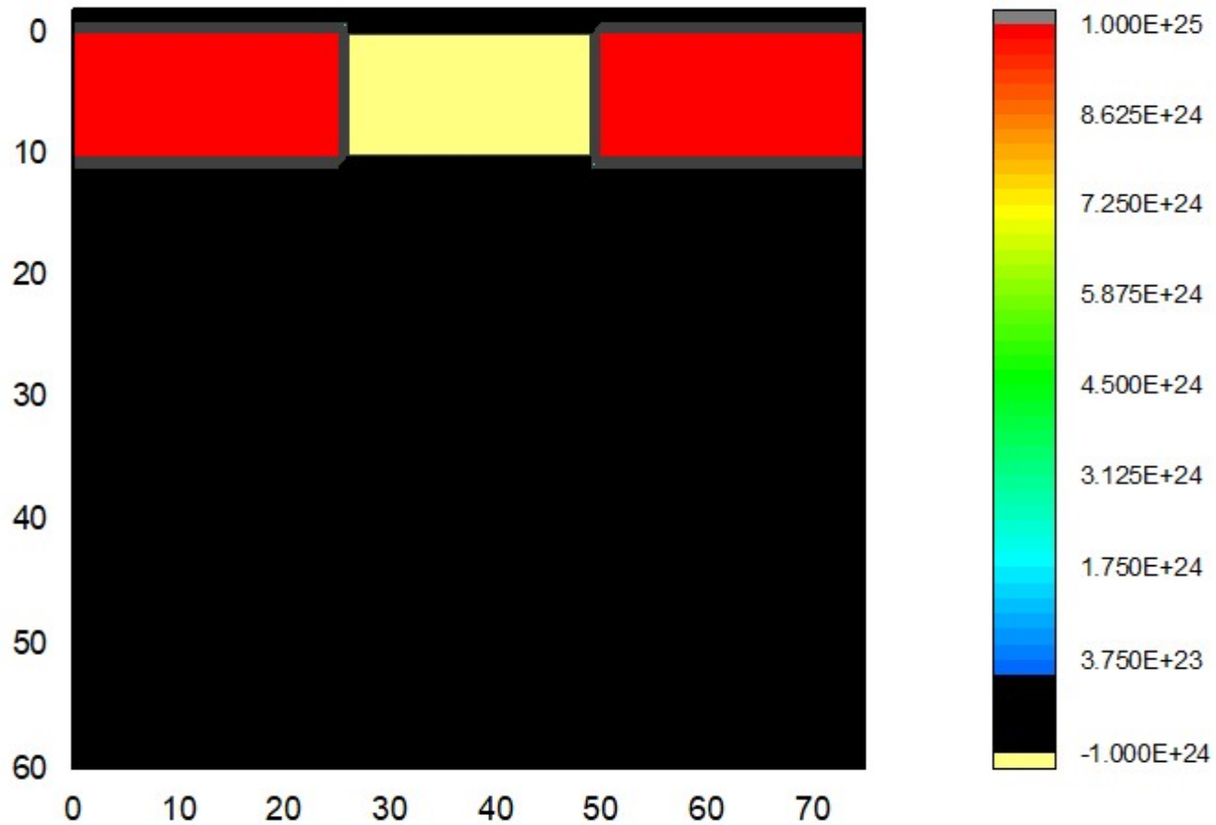

FDSOI MOSFET

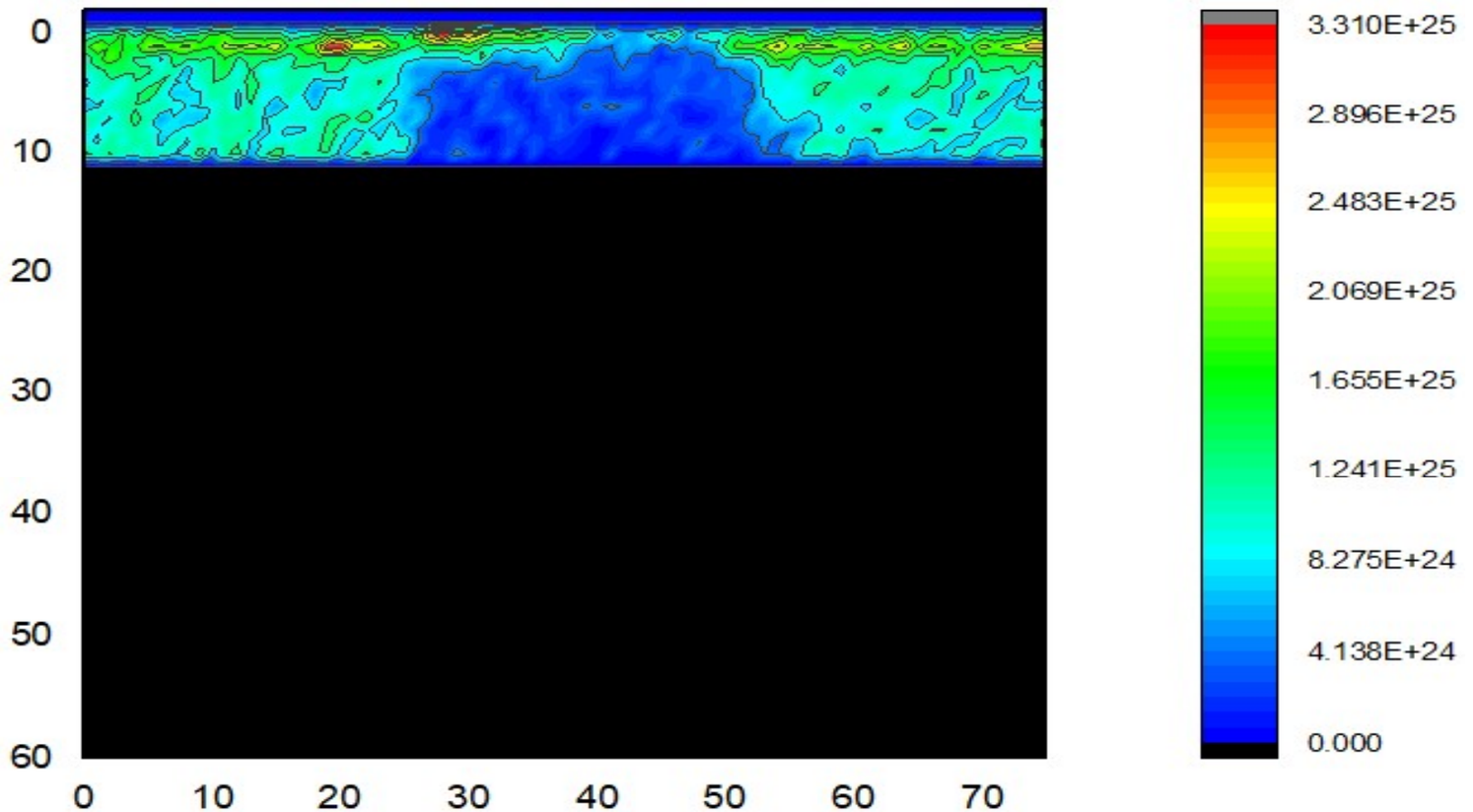

FDSOI MOSFET RESULTS

	Nodes (nm)	14nm	10nm	7nm	14nm	10nm	7nm
Structure Parameters		Single Gate			Double Gate		
	L_{eff} (nm)	22	14	10	22	14	10
	W_{eff} (nm)	10		8	10		8
	T_{ox} (nm)	1	0.85	0.75	0.75	0.85	0.75
	Doping (/cm^3)	1×10^{24}	5×10^{24}	2×10^{25}	2×10^{25}	5×10^{24}	2×10^{25}
	T_{SOI} (nm)	40	30	20	20	30	20
Device Parameters	Vth (mV)	0.3	0.22	0.2	0.2	0.4	0.5
	SS (/mV/dec)	63.3	67.9	82.9	82.9	87.4	72.2
	gm (mS/μm)	0.252	0.437	0.499	0.499	0.494	0.449

FDSOI TECHNOLOGY UP TO 7NM

Scattering Rates

- Intervalley,
- Acoustic and
- Coulomb

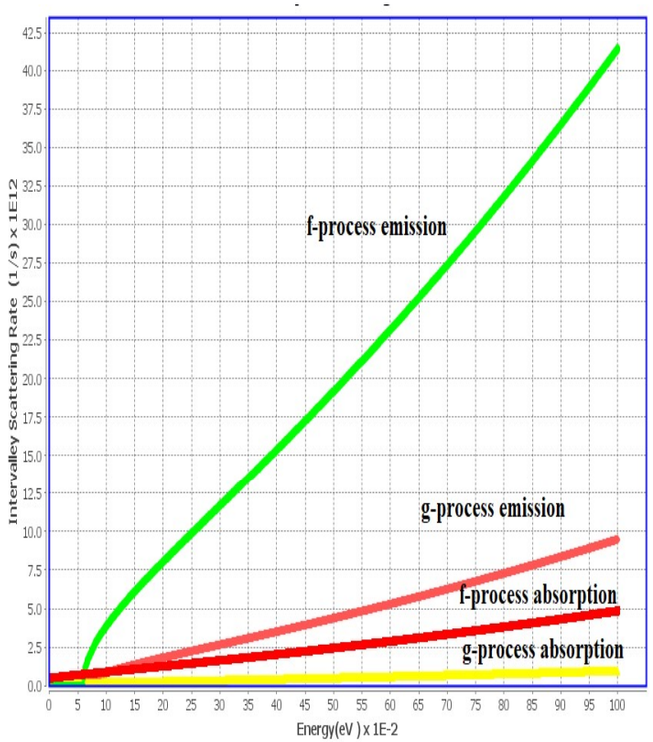

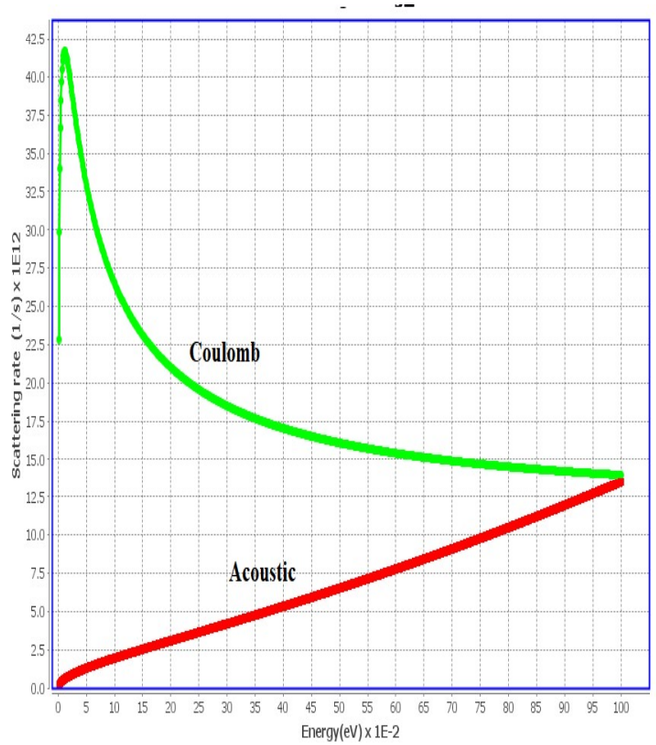

DRIFT VELOCITY

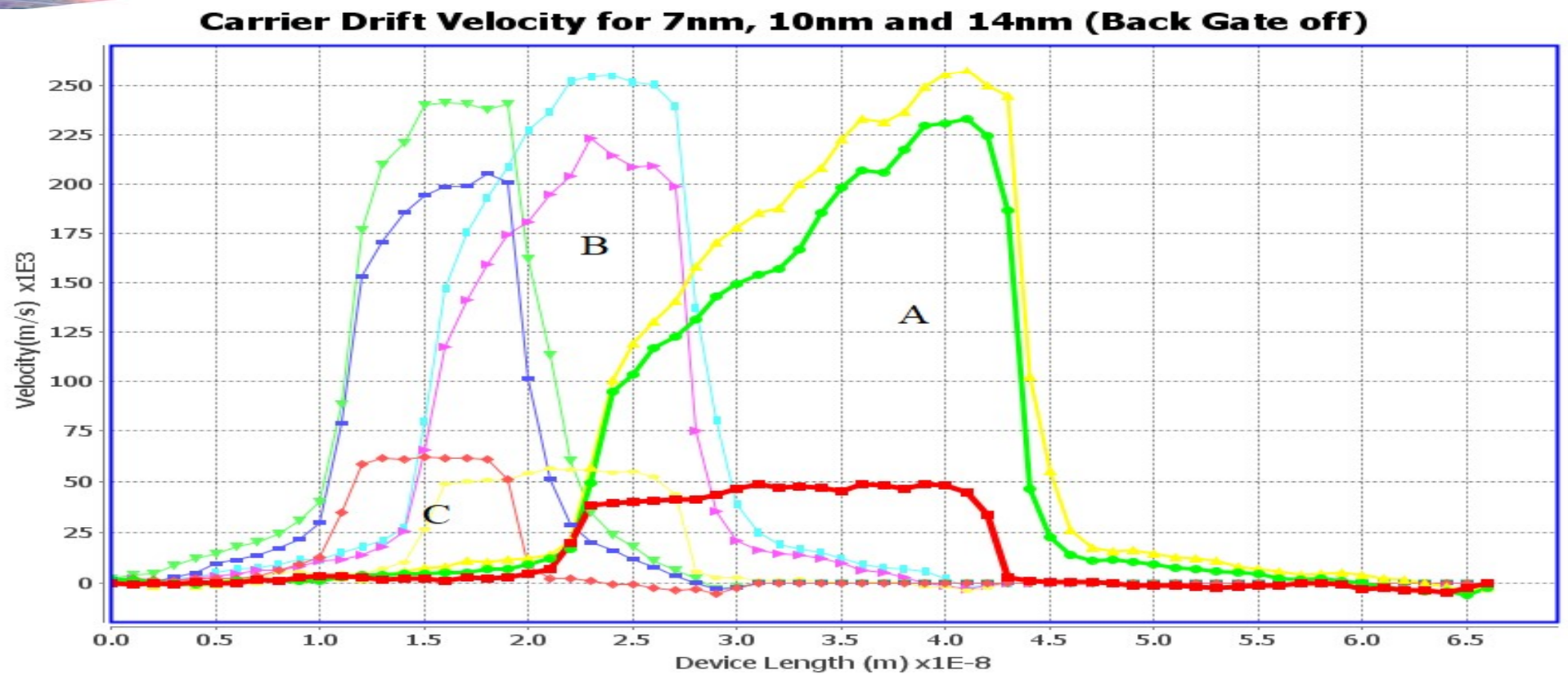

Carrier Drift velocity a) 14nm b) 10nm c) 7nm

CARRIER AVERAGE ENERGY

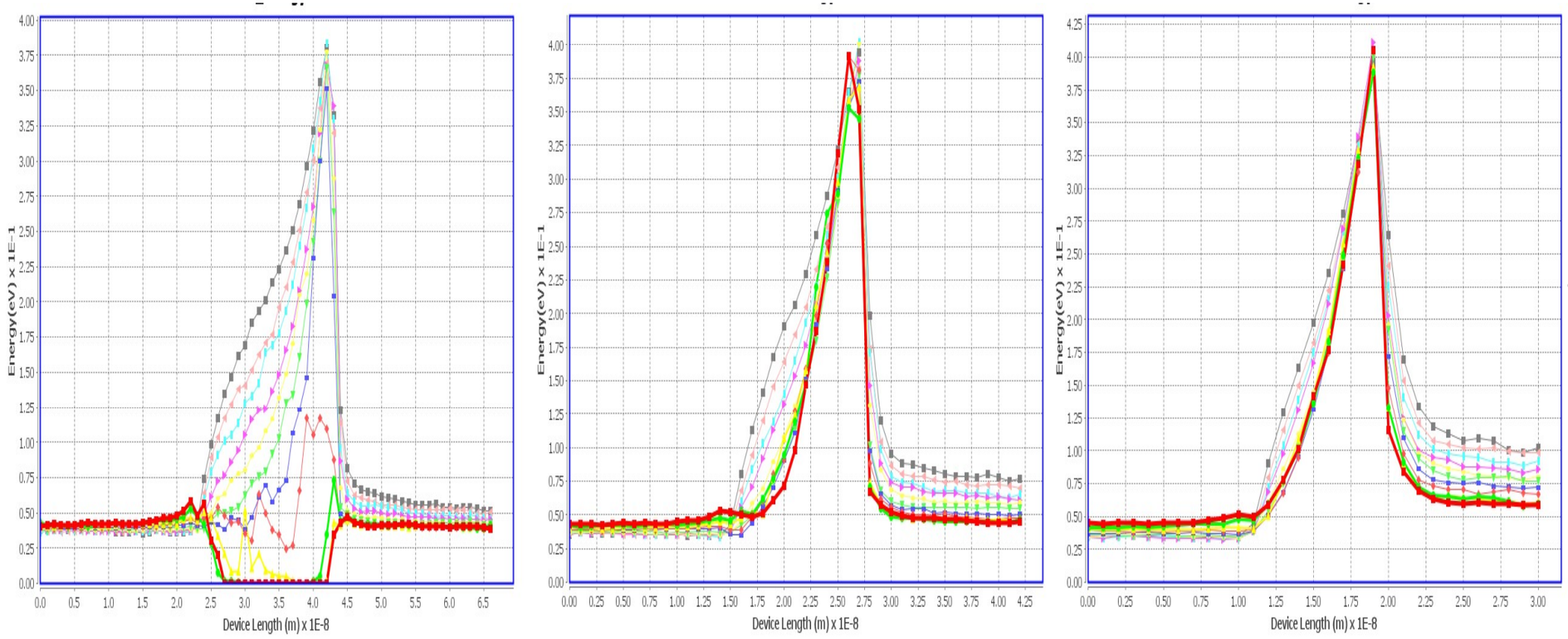

a) 14nm FDSOI MOSFET b) 10nm FDSOI MOSFET c) 7nm FDSOI MOSFET

Transfer I_d - V_g Characteristics

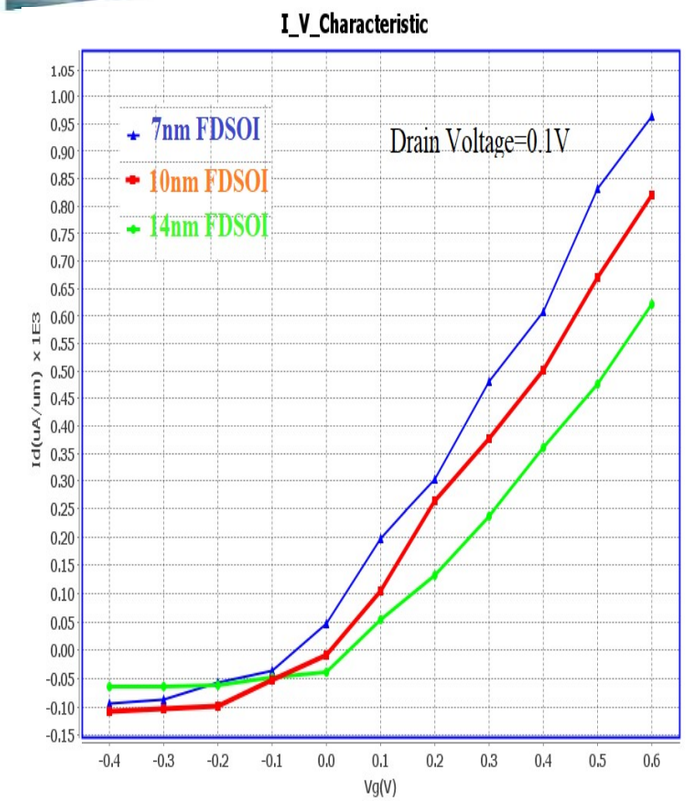

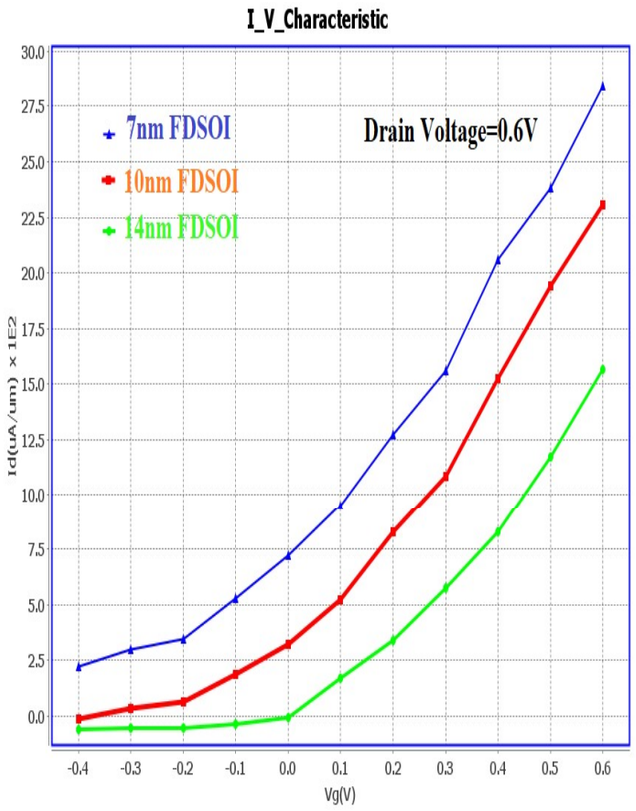

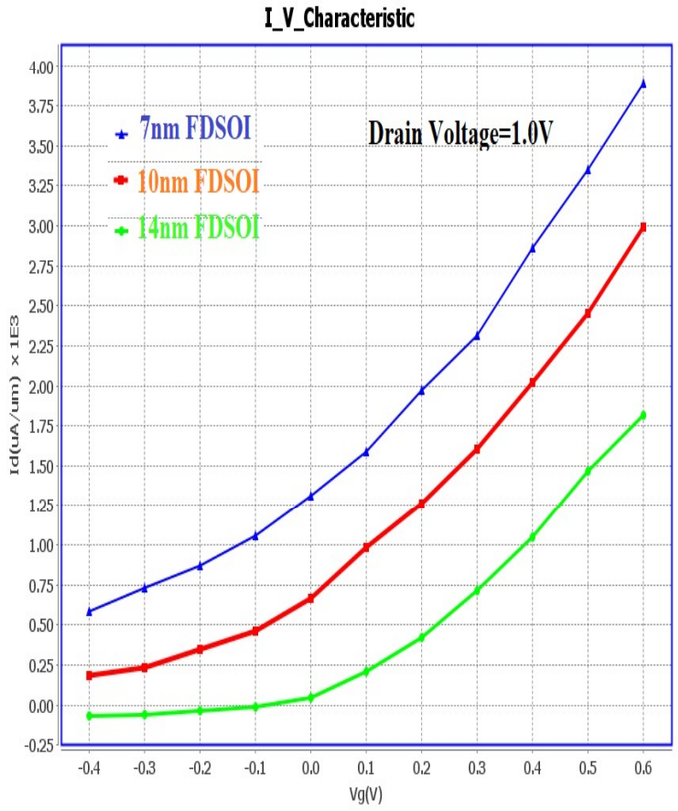

Single Gate I_d - V_d Characteristics

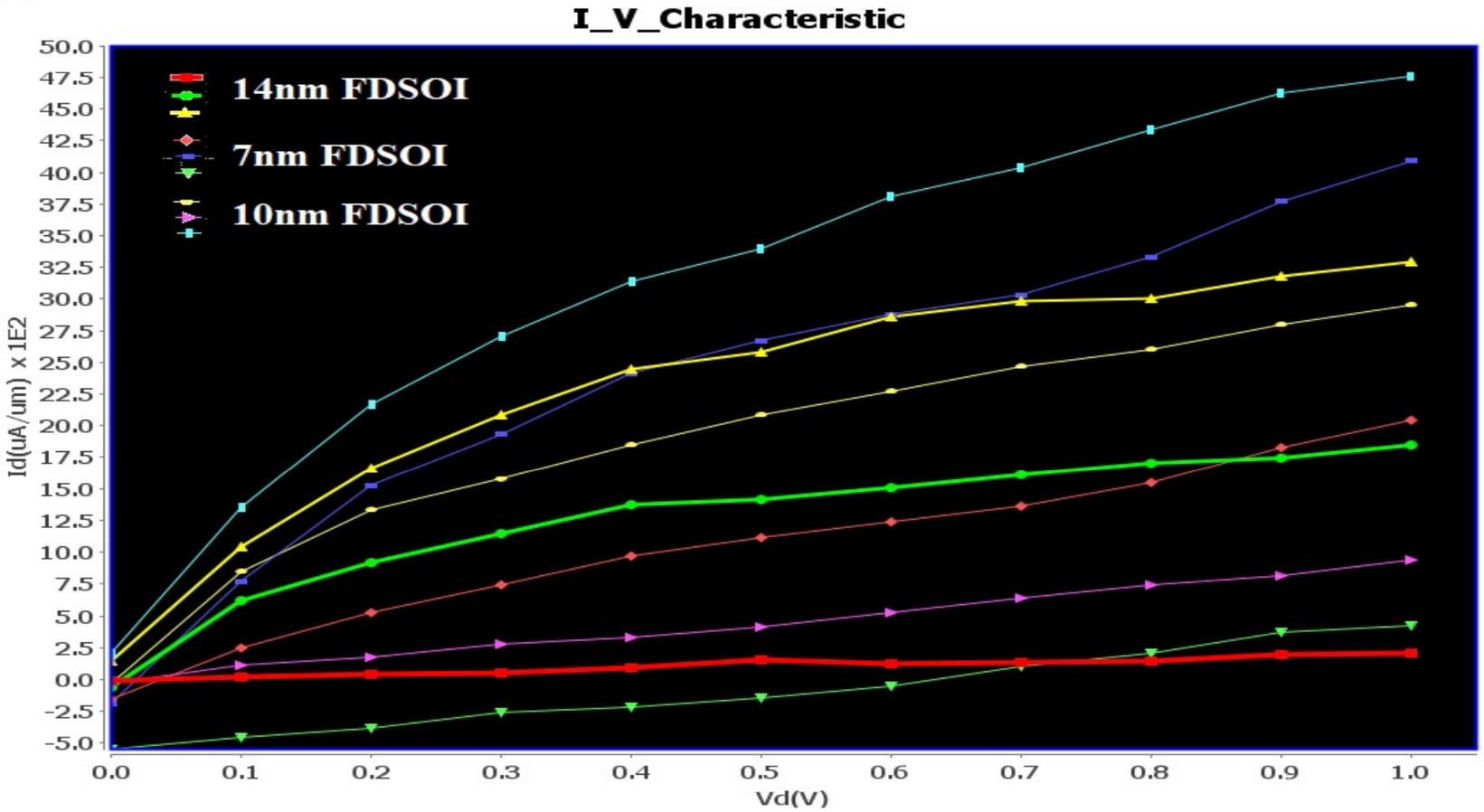

Dual Gate I - V Characteristics

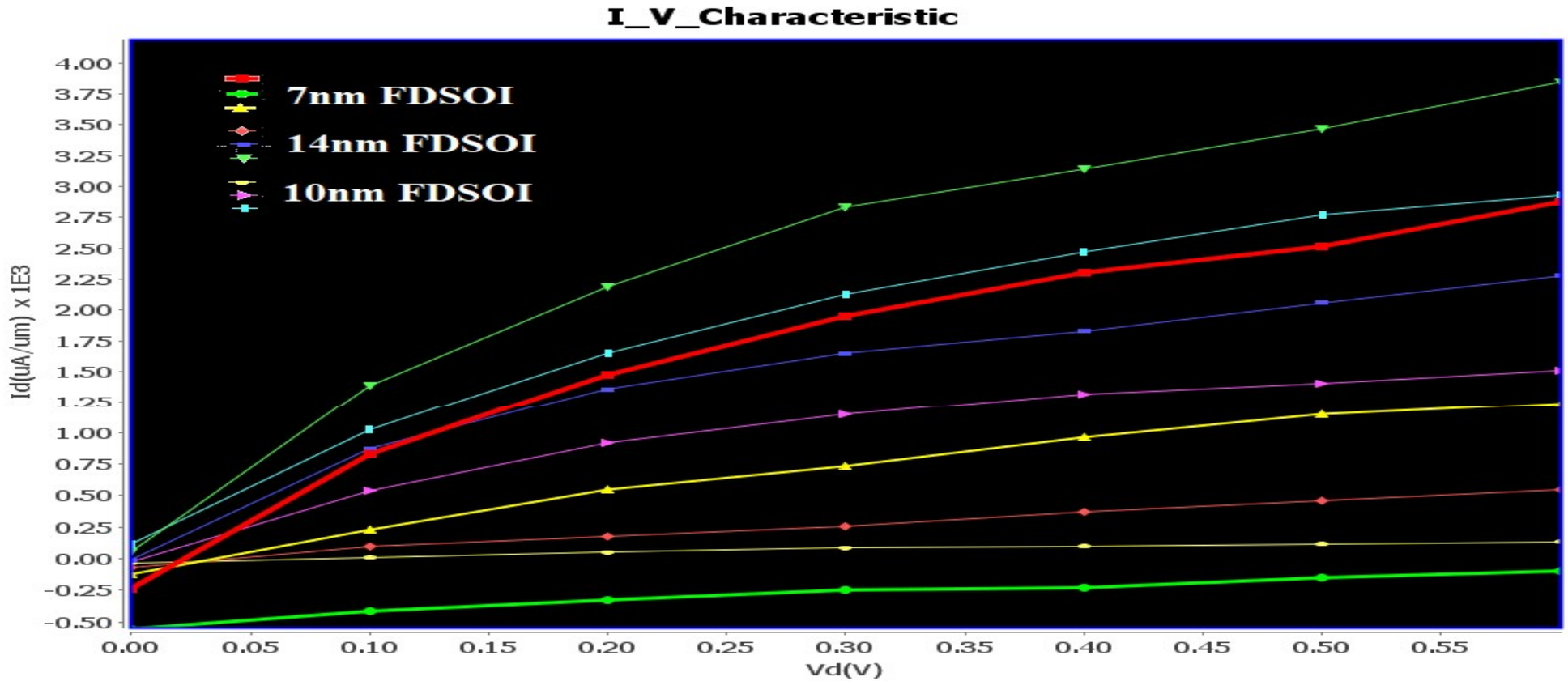

MOSFET

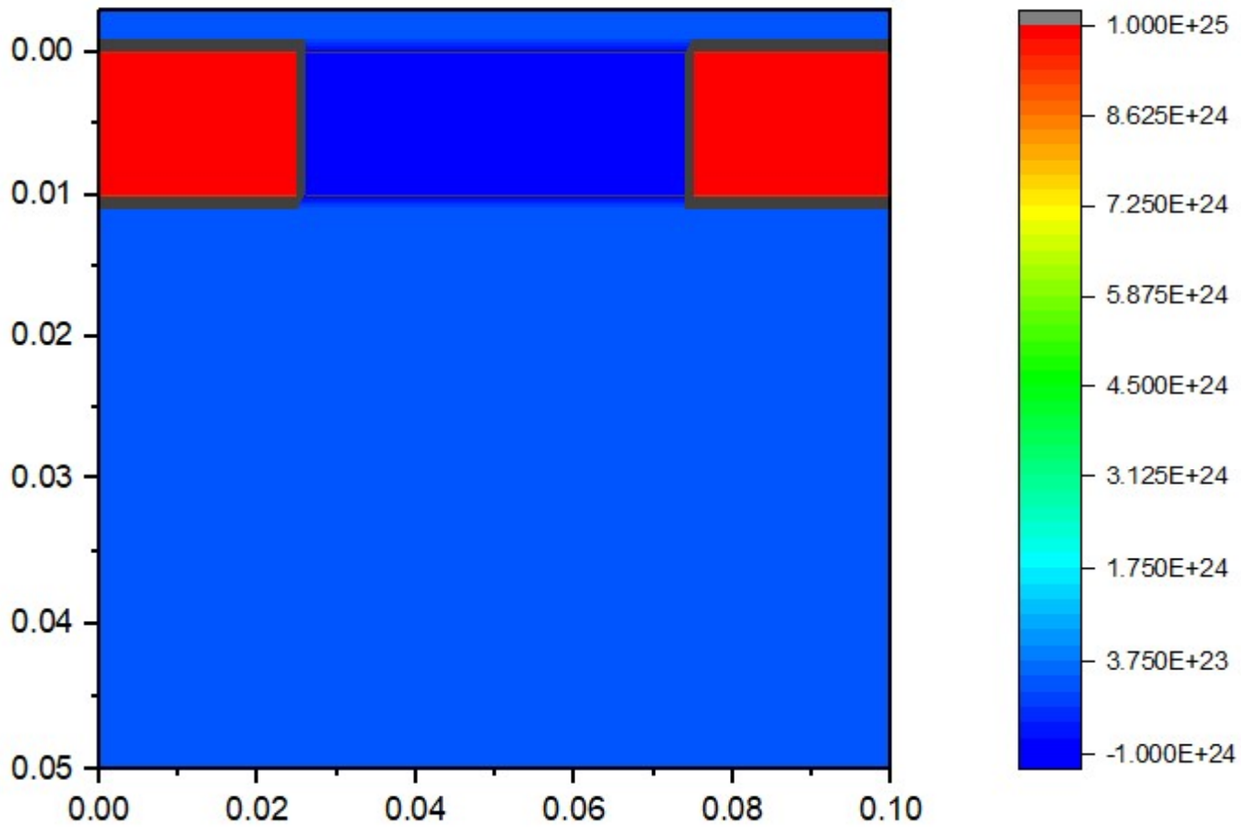
0.00
0.01
0.02
0.03
0.04
0.05
0.00
0.02
0.04
0.06
0.08
0.10
1.000E+25
8.625E+24
7.250E+24
5.875E+24
4.500E+24
3.125E+24
1.750E+24
3.750E+23
-1.000E+24

MOSFET

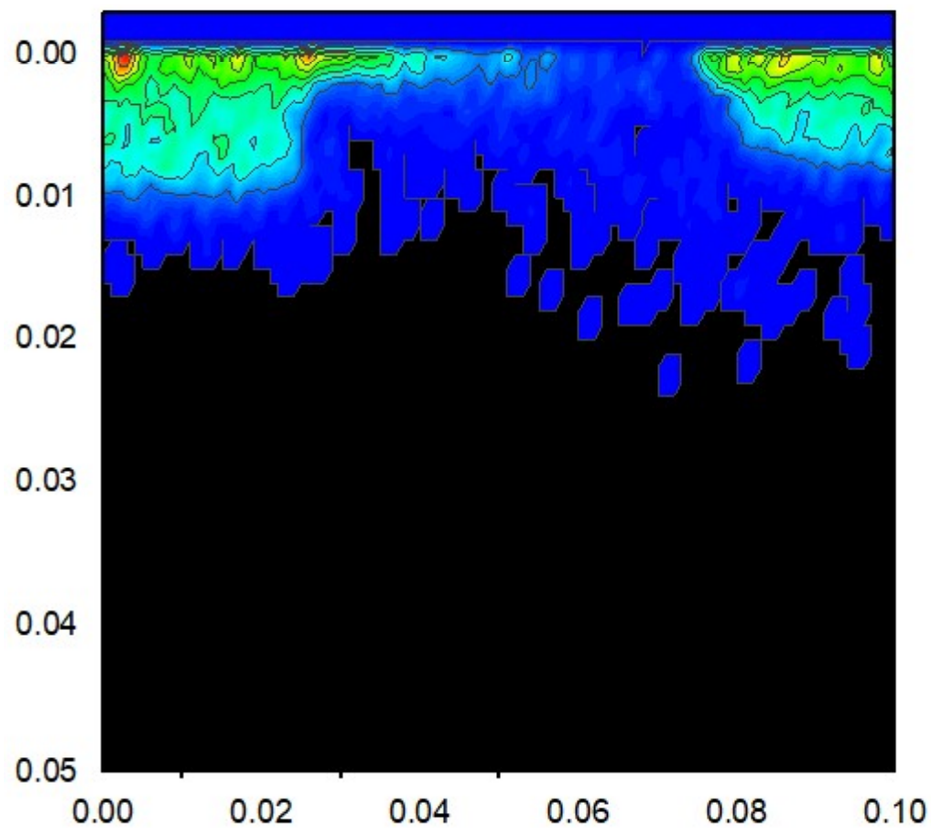
0.00
0.01
0.02
0.03
0.04
0.05
0.00
0.02
0.04
0.06
0.08
0.10
2.950E+25
2.581E+25
2.213E+25
1.844E+25
1.475E+25
1.106E+25
7.375E+24
3.688E+24
0.000

MOSFET

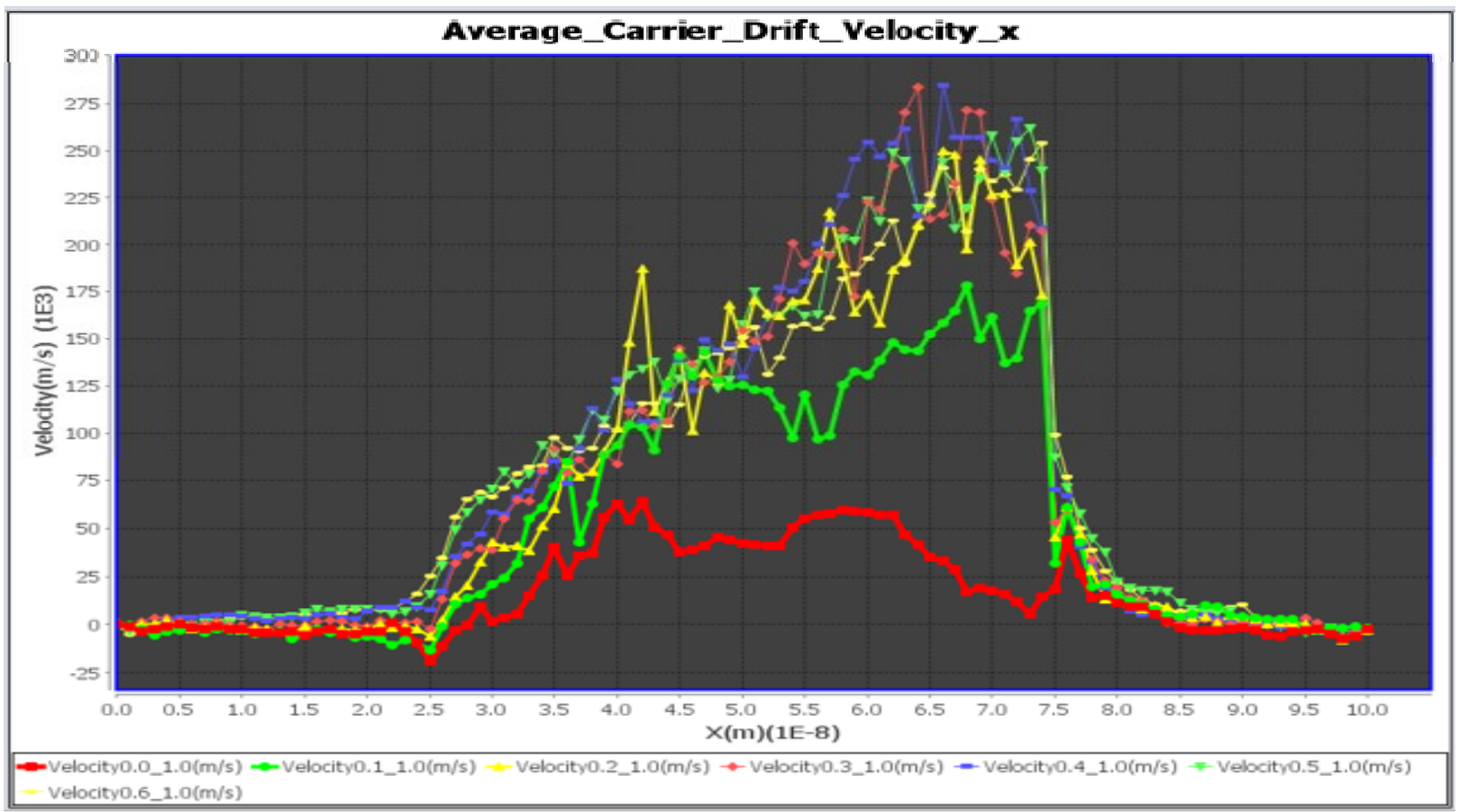
Average_Carrier_Drift_Velocity_x
Velocity(m/s) (1E3)
300
275
250
225
200
175
150
125
100
75
50
25
0
-25
0.0 0.5 1.0 1.5 2.0 2.5 3.0 3.5 4.0 4.5 5.0 5.5 6.0 6.5 7.0 7.5 8.0 8.5 9.0 9.5 10.0
X(m)(1E-8)
Velocity0.0_1.0(m/s)
Velocity0.1_1.0(m/s)
Velocity0.2_1.0(m/s)
Velocity0.3_1.0(m/s)
Velocity0.4_1.0(m/s)
Velocity0.5_1.0(m/s)
Velocity0.6_1.0(m/s)

MOSFET Transfer Characteristics

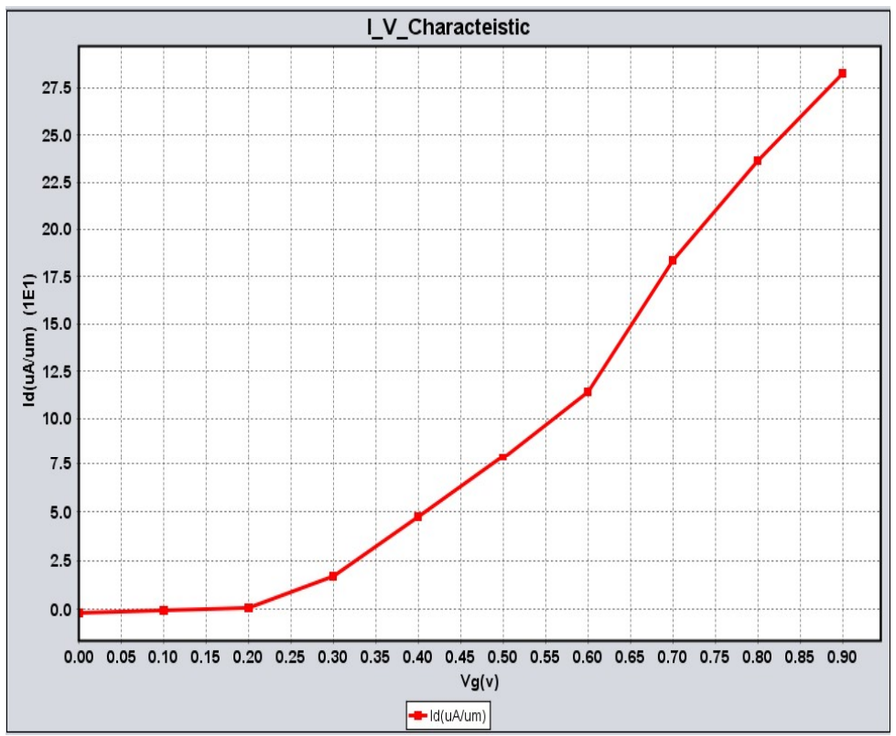

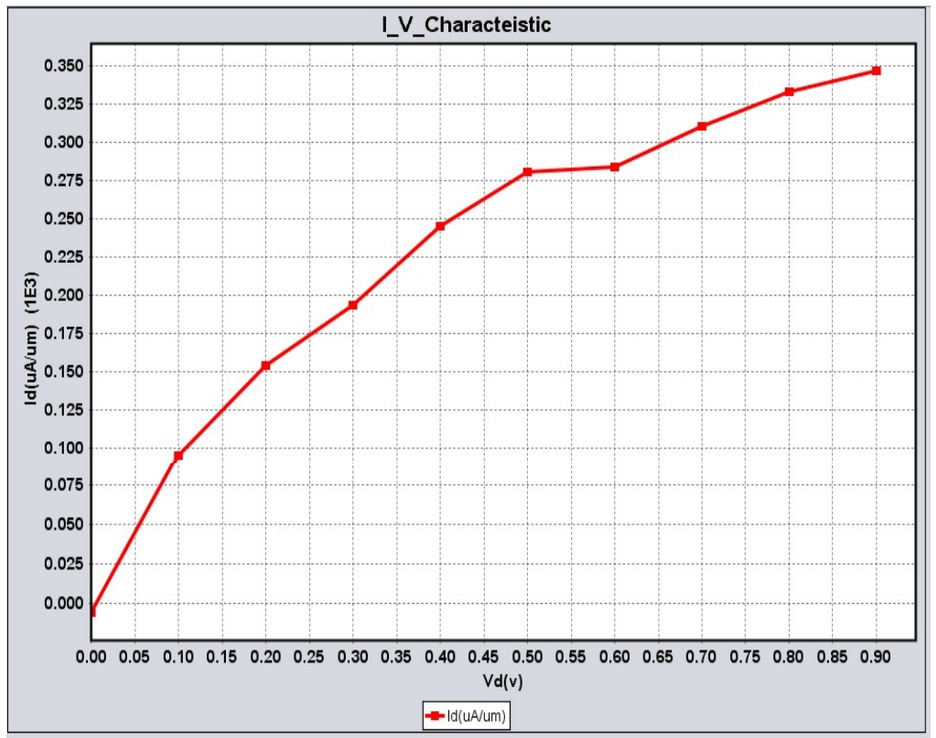

Tunneling FET

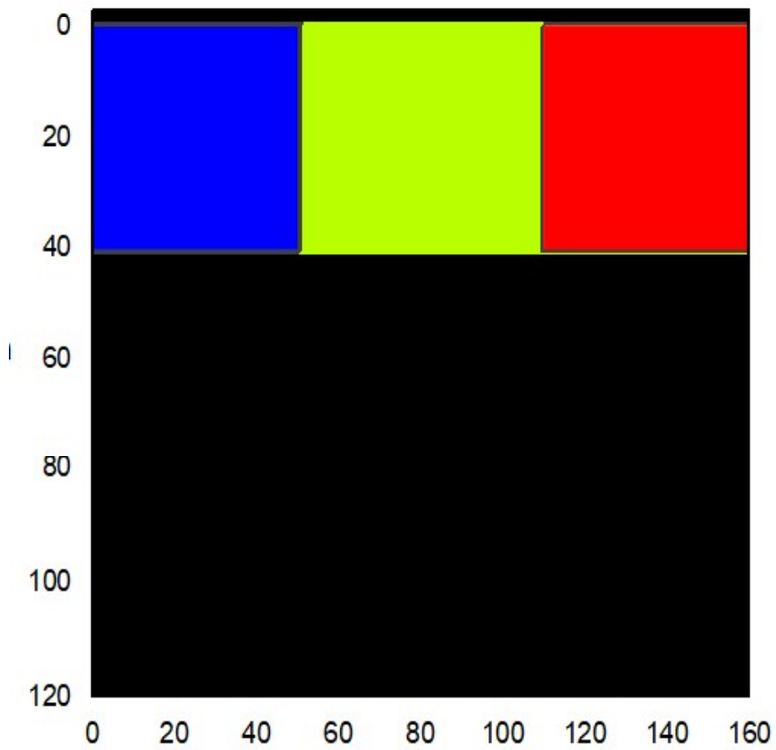

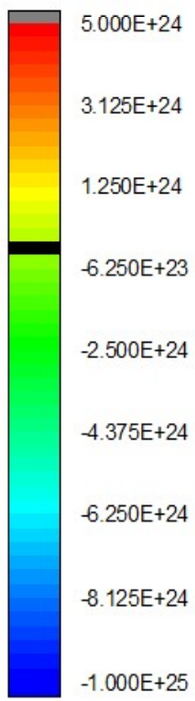

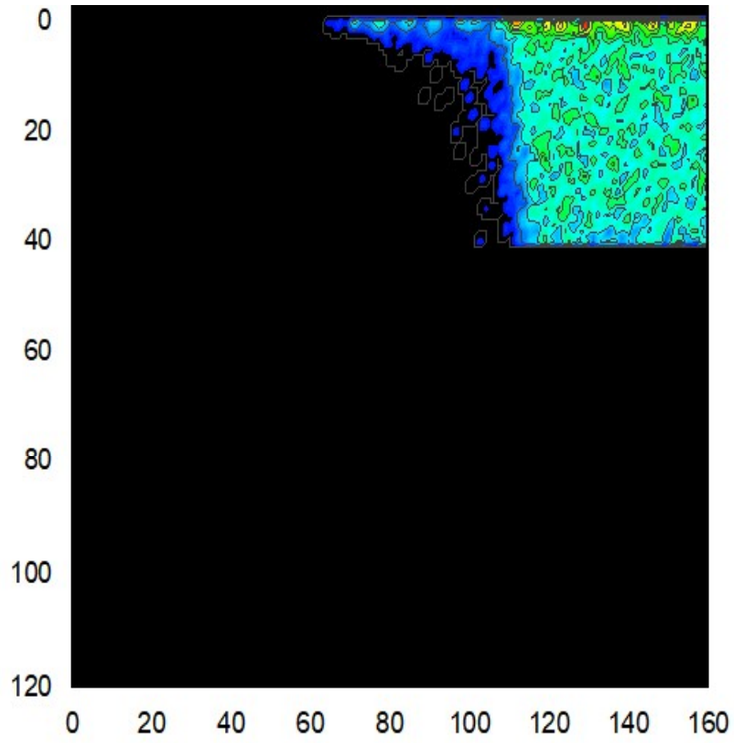

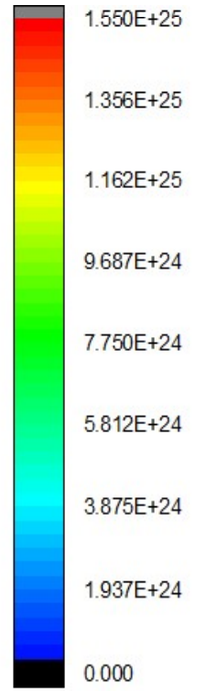

Tunneling FET

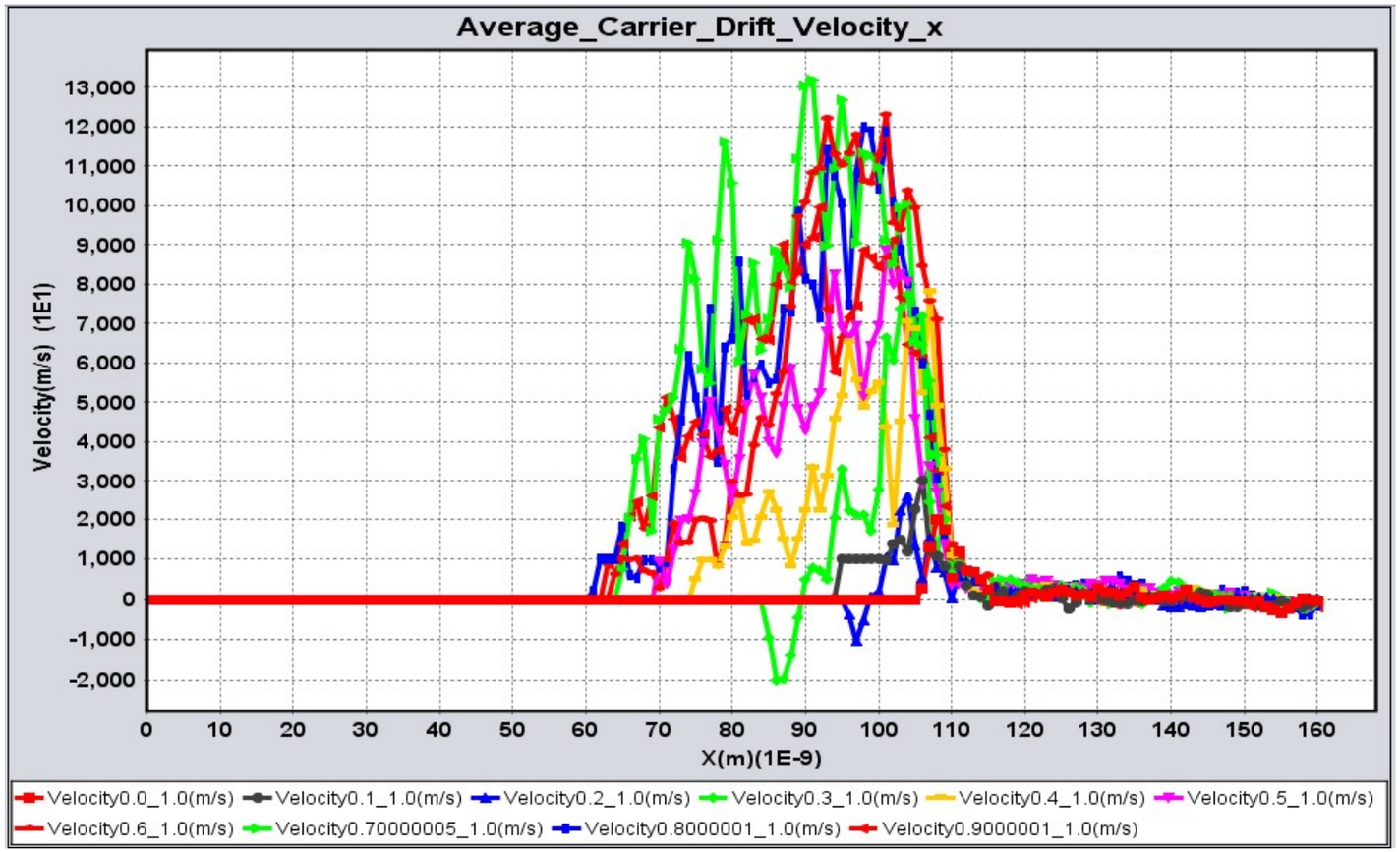

Tunneling FET Transfer Characteristics

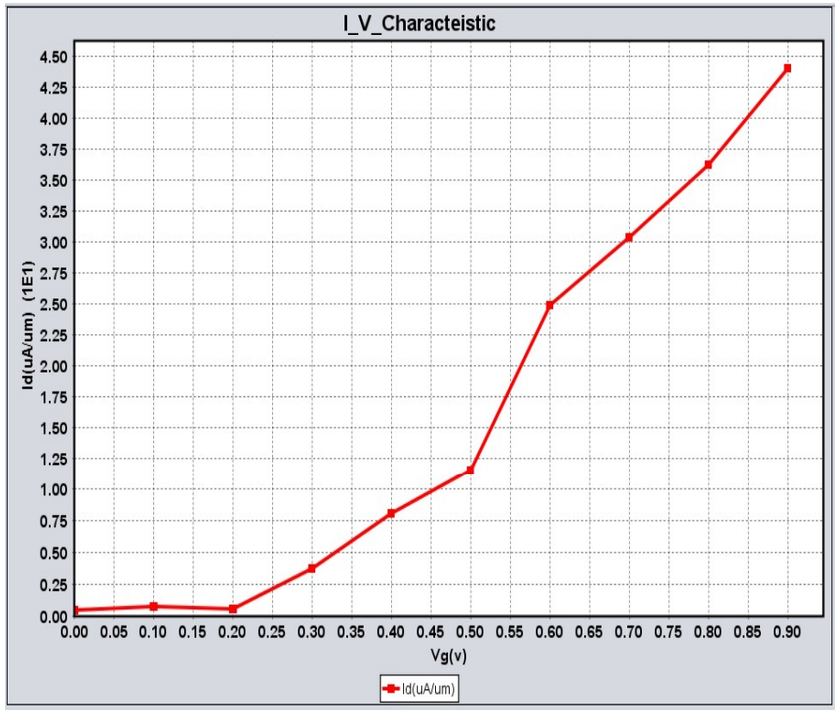

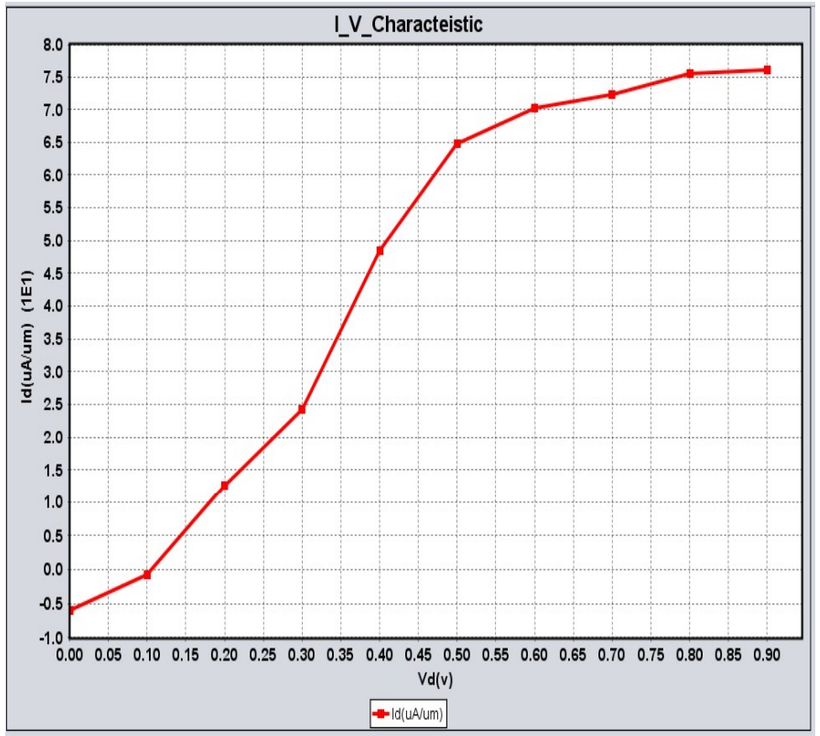

MESFET

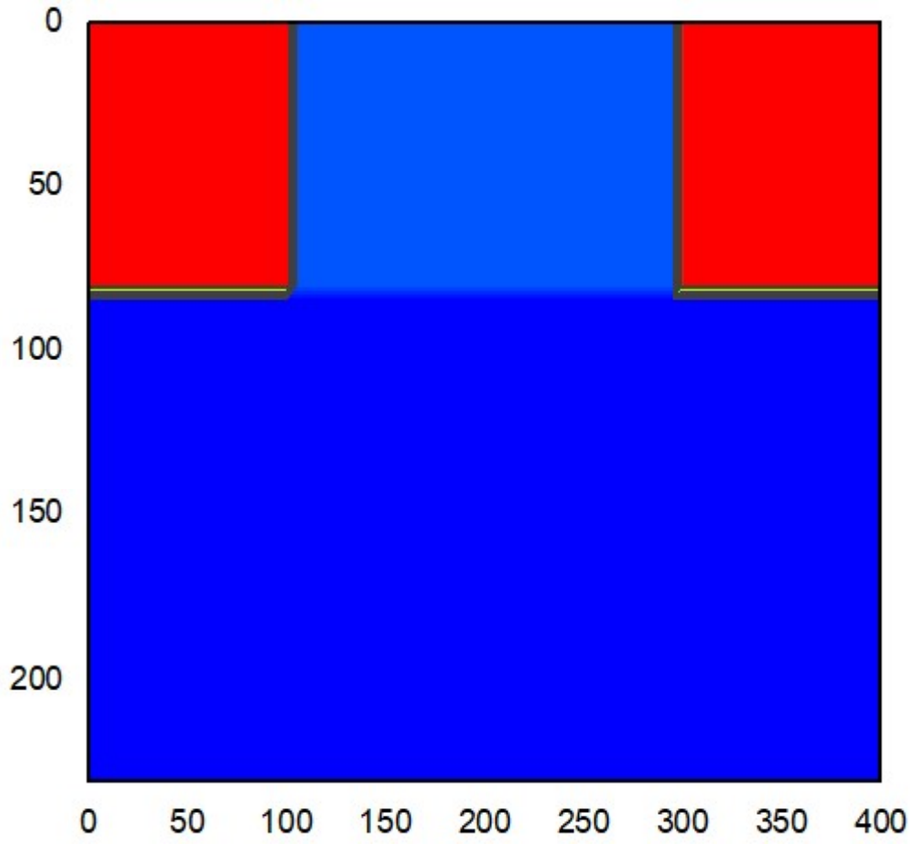
0
50
100
150
200
0
50
100
150
200
250
300
350
400

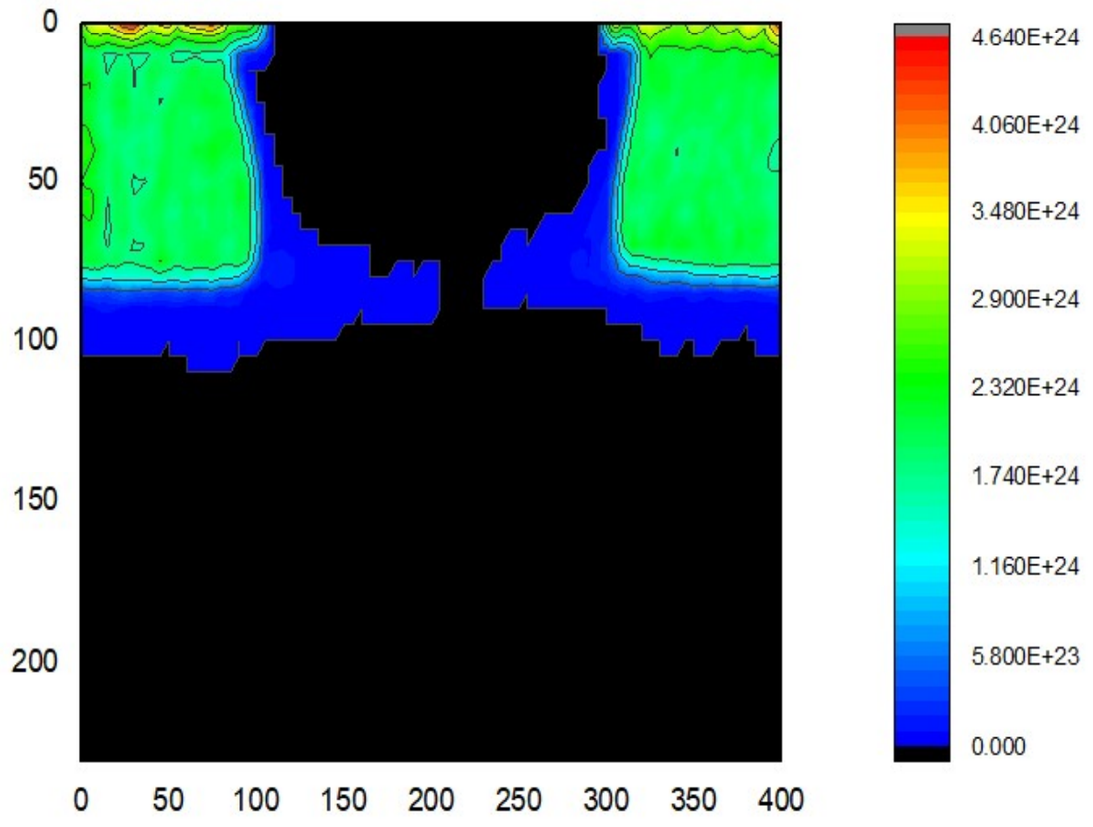
0
50
100
150
200
0
50
100
150
200
250
300
350
400
4.640E+24
4.060E+24
3.480E+24
2.900E+24
2.320E+24
1.740E+24
1.160E+24
5.800E+23
0.000

MESFET

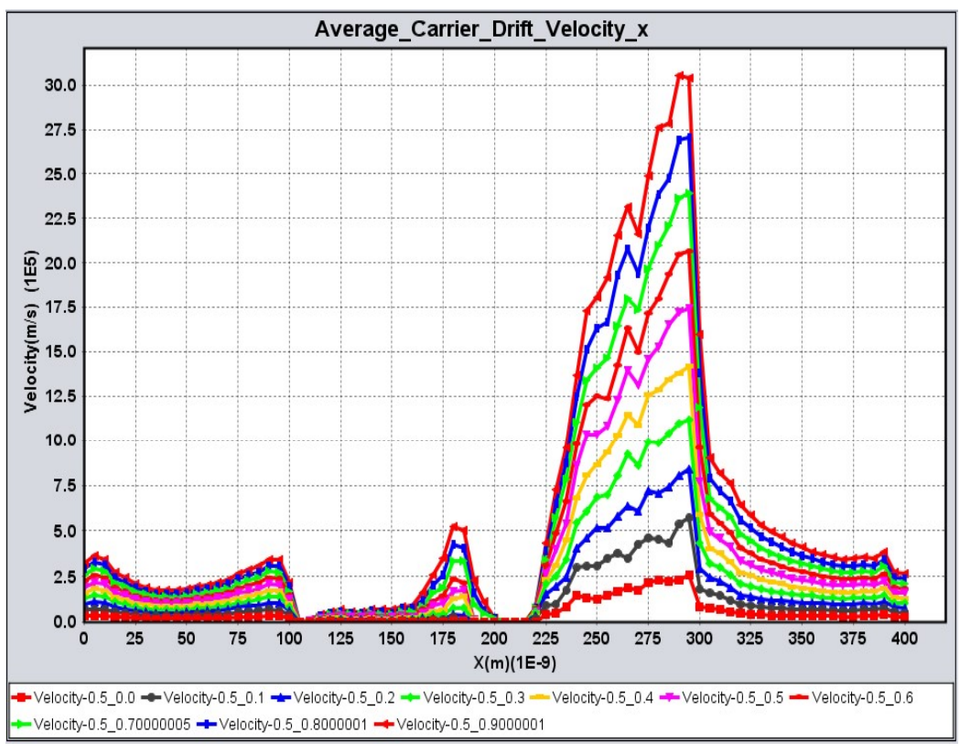
Average_Carrier_Drift_Velocity_x
Velocity(m/s) (1E5)
30.0
27.5
25.0
22.5
20.0
17.5
15.0
12.5
10.0
7.5
5.0
2.5
0.0
0 25 50 75 100 125 150 175 200 225 250 275 300 325 350 375 400
X(m)(1E-9)
Velocity-0.5_0.0
Velocity-0.5_0.1
Velocity-0.5_0.2
Velocity-0.5_0.3
Velocity-0.5_0.4
Velocity-0.5_0.5
Velocity-0.5_0.6
Velocity-0.5_0.70000005
Velocity-0.5_0.8000001
Velocity-0.5_0.9000001

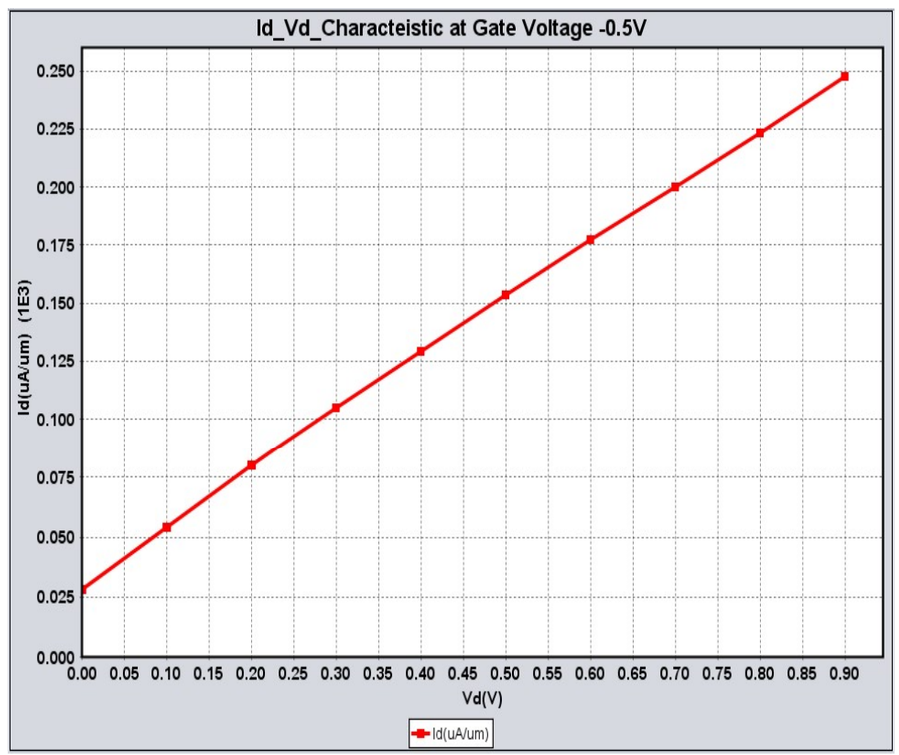
Id_Vd_Characteistic at Gate Voltage -0.5V
Id(uA/um) (1E3)
0.250
0.225
0.200
0.175
0.150
0.125
0.100
0.075
0.050
0.025
0.000
0.00 0.05 0.10 0.15 0.20 0.25 0.30 0.35 0.40 0.45 0.50 0.55 0.60 0.65 0.70 0.75 0.80 0.85 0.90
Vd(V)
Id(uA/um)

ADVANCE LICENSING & PRICE VALUE

TNL's tools support advanced and unique licensing models tailored for unique customer needs.

➢ ADVANCED LICENSING OPTIONS:

- Term-Based
- Perpetual
- TCAD Academic Suite
- 24x7 Technical Support for **Academic Institutions**

Publications

1. P.K. Saxena, numerical study of dual band (MW/LW) ir detector for Performance improvement, *Defence Science Journal*, vol. 67(2), (2017) pp. 141-148. DOI : 10.14429/dsj.67.11177
2. Praveen K. Saxena, Pankaj Srivastava, R. Trigunayat, An innovative approach for controlled epitaxial growth of GaAs in real MOCVD reactor environment, *Journal of Alloys and Compounds, vol.* 809 (2019) 151752. https://doi.org/10.1016/j.jallcom.2019.151752
3. Praveen Saxena, R. Trigunayat, Anchal Srivastava, Pankaj Srivastava, Md. Zain, R.K. Shukla, Nishant Kumar, Shivendra Tripathi, FULL ELECTRONIC BAND STURCTURE ANALYSIS OF Cd DOPED ZnO THIN FILMS DEPOSITED BY SOL-GEL SPIN COATING METHOD , II-VI US Workshop Proceedings, 2019.
4. R. K. Nanda, E. Mohapatra, T. P. Dash, P. Saxena, P. Srivastava, R. Trigutnayat, C. K. Maiti, Atomistic Level Process to Device Simulation of GaNFET Using TNL TCAD Tools, Advances in Electrical Control and Signal Systems pp 815-826, (2020), Spinger Book. https://doi.org/10.1007/978-981-15-5262-5_61
5. Sanjeev Tyagi, P. K. Saxena, Rishabh Kumar, Numerical simulation of InxGa1−xAs/InP PIN photodetector for optimum performance at 298 K, Optical and Quantum Electronics (2020) 52:374. https://doi.org/10.1007/s11082-020-02488-1
6. Praveen K Saxena *at. el.,* An Innovative Model for Electronic Band Structure Analysis of doped and un-doped ZnO, *Journal of Electronic Materials Accepted for publication.*
7. Anshika Srivastava, Anshu Saxena, Praveen K. Saxena, F. K.Gupta, Priyanka Shakya, *at. el*.**,** An innovative technique for electronic transport model of group-III nitrides, ***Scientific Reports nature research*** (2020) **10**:18706.

Thank You

Contact us

+91-983-915-1284

info@technextlab.com

Lucknow 226 003, INDIA

www.technextlab.com